MINISTRY OF EDUCATION AND SCIENCE OF UKRAINE
KYIV NATIONAL UNIVERSITY OF TECHNOLOGIES AND DESIGN
Faculty of Chemical and Biopharmaceutical Technologies
Department of Biotechnology, Leather and Fur

QUALIFICATION THESIS

on the topic **Cell characteristics of exopolysaccharides from four marine bacteria and microscopic observation**

First (Bachelor's) level of higher education

Specialty 162 "Biotechnology and Bioengineering"

Educational and professional program "Biotechnology"

Completed: student of group BEBT-21
Ju Yiting

Scientific supervisor
Olena Okhmat, Ph.D., Assoc. Prof.

Reviewer
Iryna Voloshyna, Ph.D., Assoc. Prof.

Kyiv 2025

KYIV NATIONAL UNIVERSITY OF TECHNOLOGIES AND DESIGN

Faculty: Chemical and Biopharmaceutical Technologies
Department: Biotechnology, Leather and Fur
First (Bachelor's) level of higher education
Specialty: 162 Biotechnology and Bioengineering
Educational and professional program Biotechnology

APPROVE
Head of Biotechnology, Leather and Fur Department, Professor,
Dr. Sc., Prof.
_____Olena MOKROUSOVA
«___»_____2025

ASSIGNMENTS
FOR THE QUALIFICATION THESIS
Ju Yiting

1. Thesis topic **Cell characteristics of exopolysaccharides from four marine bacteria and microscopic observation**

Scientific supervisor Ph.D., Asos. Prof. Olena OKHMAT

approved by the order of KNUTD “23” May 2025, № 109-уч

2. Initial data for work: assignments for qualification thesis, scientific literature on the topic of qualification thesis, materials of Pre-graduation practice

3. Content of the thesis (list of questions to be developed): literature review; object, purpose, and methods of the study; experimental part; conclusions

4. Date of issuance of the assignments 05.03.2025

WORK CALENDAR

№	The name of the stages of the qualification thesis	Terms of performance of stage	Note on performance
1	Introduction	until 11 April 2025	
2	Chapter 1. Literature review	until 20 April 2025	
3	Chapter 2. Object, purpose, and methods of the study	until 30 April 2025	
4	Chapter 3. Experimental part	until 11 May 2025	
5	Conclusions	until 15 May 2025	
6	Draw up a bachelor's thesis (final version)	until 25 May 2025	
7	Submission of qualification work to the supervisor for feedback	until 27 May 2025	
8	Submission of bachelor's thesis to the department for review (14 days before the defense)	28 May 2025	
9	Checking the bachelor's thesis for signs of plagiarism (10 days before the defense)		Similarity coefficient ____% Citation rate ____%
10	Submission of bachelor's thesis for approval by the head of the department (from 7 days before the defense)		

I am familiar with the task:

Student _____ Ju Yiting

Scientific supervisor _____ Olena OKHMAT

ABSTRACT

Ju Yiting. Cell characteristics of exopolysaccharides from four marine bacteria and microscopic observation. – Manuscript.

Qualification thesis on the specialty 162 «Biotechnology and Bioengineering». – Kyiv National University of Technologies and Design, Kyiv, 2025.

In the field of microbiology, bacterial exopolysaccharide (EPS) have become a research hotspot due to their unique biological functions and broad application potential. However, EPS produced by different bacteria exhibit significant variations in yield, structure, and functionality, making an in-depth investigation of their properties crucial for unlocking their potential applications.

This study selected four representative marine bacteria as research subjects, aiming to determine their growth curves during the synthesis of extracellular polysaccharides and to dynamically understand the relationship between b acterial growth and extracellular polysaccharide synthesis. Meanwhile, laser confocal microscopy and transmission electron microscopy techniques were employed to analyze the structural characteristics of extracellular pol ysaccharides at the microscopic level, providing a theoretical basis for revealing the synthesis mechanism of extracellular polysaccharides and optimizing the production process.

The research results indicated that under the culture condition of 25^{o}C, the four marine bacteria had similar physiological characteristics, entering the exponential growth phase at 2h-4h and the stable growth phase at 18h-24h. At the same time, the interaction between marine bacteria and extracellular polysaccharides showed asignificant time dependence, closely related to the four growth periods of bacteria. However, the extracellular polysaccharide yields during the stable growth phase varied among the four strains, ranging approximately from 0.18 g/L to 0.4 g/ L. This study analyzed 48 laser confocal microscopy images and 6 transmission electron microscopy images of Hao2018, elucidating the cellular characteristics of extracellular polysaccharides at the microscopic level. Through systematic research, it is expected to lay a foundation for the efficient development and utilization of bacterial extracellular

polysaccharides and promote the development of related industries.

Key words :Marine Bacteria; Exopolysaccharide; Laser Confocal Microscopy; Transmission Electron Microscopy

TABLE OF CONTENTS

INTRODUCTION

As the most vast and unique ecosystem on earth, the ocean contains rich and diverse microbial resources, of which marine bacteria are an important part. These bacteria can synthesize and secrete extracellular polysaccharide (EPS) in the process of growth and metabolism, which not only plays a key role in the physiological process of bacterial survival, adhesion, defense and other processes, but also shows great application potential in the fields of food, medicine, chemical industry and the like due to the unique chemical structure and diverse biological activities[1]. There are significant differences in the structure of exopolysaccharides from different sources and species of marine bacteria. In-depth study of its structural characteristics is the basis and key to reveal its functional mechanism and develop high value-added products.

Structure determines function and clarifying the structural characteristics of marine bacterial exopolysaccharides is crucial for understanding its nature and mining application value. The mobility of the marine and other aquatic environments forces some organisms to have corresponding viscous structures or substances to ensure that marine organisms have a relatively stable ecological environment[2]. Traditional chemical analysis methods, such as high-performance liquid chromatography and NMR, can analyze the monosaccharide composition and glycosidic bond linkage of polysaccharides from the molecular level, but it is difficult to visually represent the morphology and aggregation state of polysaccharides at the micro-scale. With the continuous development of microscopy, laser confocal microscopy (CLSM) and transmission electron microscopy (TEM) have provided new perspectives for the study of the structure of polysaccharides. Laser scanning confocal microscope is a set of observation, analysis and output system which uses laser as the light source, the conjugate focusing principle and device on the basis of the traditional optical microscope, and uses the computer to process the digital image of the observed object. Through the laser scanning confocal microscope, the observation sample can be subjected to tomographic scanning and imaging, and the three-dimensional space structure of the observation sample can be observed and analyzed without damage, so

that the laser scanning confocal microscope has advantages which are incomparable to those of an electron microscope and a common light microscope33. TEM, through electron beam passing through the samples, presented the ultrastructure of exopolysaccharides with extremely high resolution, and observed the molecular chain conformation, aggregation state and nano-scale fine structure characteristics of polysaccharides. The two complemented each other, providing a powerful tool for comprehensive analysis of the structure of exopolysaccharides[4].

At present, although there have been some reports on the structure of marine bacterial exopolysaccharides, systematic research on the exopolysaccharides of specific strains is still relatively scarce. In this study, four representative marine bacteria were selected to deeply explore the structural characteristics of exopolysaccharides using comprehensive chemical analysis methods and microscopy techniques such as CLSM and TEM, aiming to comprehensively analyze the structure of exopolysaccharides from both the molecular level and the micro-morphology, provide the theoretical basis and technical support for revealing the structure-activity relationship and developing new marine polysaccharide materials, and also hope to open a new path for the efficient utilization of marine microbial resources.

CHAPTER 1
LITERATURE REVIEW

As the most vast and unique ecosystem on earth, the ocean contains rich and diverse microbial resources, of which marine bacteria are an important part. These bacteria can synthesize and secrete extracellular polysaccharide (EPS) in the process of growth and metabolism, which not only plays a key role in the physiological process of bacterial survival, adhesion, defense and other processes, but also shows great application potential in the fields of food, medicine, chemical industry and the like due to the unique chemical structure and diverse biological activities[1]. There are significant differences in the structure of exopolysaccharides from different sources and species of marine bacteria. In-depth study of its structural characteristics is the basis and key to reveal its functional mechanism and develop high value-added products.

Structure determines function and clarifying the structural characteristics of marine bacterial exopolysaccharides is crucial for understanding its nature and mining application value. The mobility of the marine and other aquatic environments forces some organisms to have corresponding viscous structures or substances to ensure that marine organisms have a relatively stable ecological environment[2]. Traditional chemical analysis methods, such as high-performance liquid chromatography and NMR, can analyze the monosaccharide composition and glycosidic bond linkage of polysaccharides from the molecular level, but it is difficult to visually represent the morphology and aggregation state of polysaccharides at the micro-scale. With the continuous development of microscopy, laser confocal microscopy (CLSM) and transmission electron microscopy (TEM) have provided new perspectives for the study of the structure of polysaccharides. Laser scanning confocal microscope is a set of observation, analysis and output system which uses laser as the light source, the conjugate focusing principle and device on the basis of the traditional optical microscope, and uses the computer to process the digital image of the observed object. Through the laser scanning confocal microscope, the observation sample can be subjected to tomographic scanning and imaging, and the three-dimensional space

structure of the observation sample can be observed and analyzed without damage, so that the laser scanning confocal microscope has advantages which are incomparable to those of an electron microscope and a common light microscope33. TEM, through electron beam passing through the samples, presented the ultrastructure of exopolysaccharides with extremely high resolution, and observed the molecular chain conformation, aggregation state and nano-scale fine structure characteristics of polysaccharides. The two complemented each other, providing a powerful tool for comprehensive analysis of the structure of exopolysaccharides[4].

At present, although there have been some reports on the structure of marine bacterial exopolysaccharides, systematic research on the exopolysaccharides of specific strains is still relatively scarce. In this study, four representative marine bacteria were selected to deeply explore the structural characteristics of exopolysaccharides using comprehensive chemical analysis methods and microscopy techniques such as CLSM and TEM, aiming to comprehensively analyze the structure of exopolysaccharides from both the molecular level and the micro-morphology, provide the theoretical basis and technical support for revealing the structure-activity relationship and developing new marine polysaccharide materials, and also hope to open a new path for the efficient utilization of marine microbial resources.

1.1 Overview of marine bacterial exopolysaccharides

Marine bacterial exopolysaccharides are a class of high molecular weight polysaccharide compounds secreted by certain bacteria in the marine environment, with complex chemical structures and diverse biological activities. These polysaccharides are usually formed by monosaccharide units connected by glycosidic bonds and may contain modification groups such as sulfate groups, acetyl groups or carboxymethyl groups, giving them unique physicochemical properties, such as high viscosity, emulsification and gel-forming ability. In the ecological sense, marine bacterial exopolysaccharides not only serve as the main component of bacterial biofilm to help bacteria attach to the surface and form a stable microenvironment6, but also to withstand extreme environmental pressure, such as high salt, low temperature or high

pressure, etc. In addition, the polysaccharides have wide application prospects in the fields of biomedicine, food industry, environmental repair and the like, for example, as antioxidants, antitumor drug carriers or heavy metal adsorbents. In recent years, with the in-depth exploration of marine microbial resources, marine bacterial exopolysaccharides have become a hot research topic due to their structural novelty and functional diversity. However, their large-scale production and application still face challenges such as optimization of culture conditions, structural analysis and functional mechanism research.

1.2 Overview of laser confocal microscopy (LSCM)

1.2.1 Introduction to LSCM

Laser scanning confocal microscope (LSCM) is a high-resolution optical imaging technology, which realizes three-dimensional high-definition imaging of samples by combining a laser light source, a confocal optical system and computer image processing. Compared with the traditional optical microscope, its core advantage lies in the fact that the pinhole device is used to filter the stray light out of the focal plane, thus significantly improving the signal-to-noise ratio and axial resolution of the image, and thus obtaining a clearer tomographic image. The technique can be used for non-invasive observation of fluorescently labeled samples and is widely applied to such fields as cell biology, neuroscience and materials science, such as dynamic tracking of organelles, protein localization analysis and three-dimensional tissue structure reconstruction. In addition, the laser confocal microscope can also combine multiple fluorescent probes to realize multicolor fluorescence imaging and even carry out real-time dynamic monitoring of living cells. Although this technique has high resolution and three-dimensional imaging capability, its equipment cost is high, and the requirements for fluorescence labeling and preparation of samples are strict. Therefore, the advantages and disadvantages of this technique should be weighed according to the research requirements during application. In recent years, with the development of super-resolution microscopy, laser confocal microscopy still occupies an important position in the field of scientific research due to its stability and versatility.

1.2.2 Benefits of LSCM

Laser confocal microscopy has significant advantages in biomedical and material science research, mainly reflected in its excellent optical resolution and three-dimensional imaging capability. Compared with the traditional wide-field fluorescence microscope, the technology effectively eliminates the interference of defocused light through the confocal pinhole, and significantly improves the signal-to-noise ratio of the image. It is especially suitable for high-definition tomography with thick samples. Its optical slicing capability allows for non-destructive layer-by-layer imaging of samples, combined with three-dimensional reconstruction software to accurately analyze the spatial distribution of complex biological structures or material surface topography. In addition, the laser confocal microscope has the function of multi-channel fluorescence detection, and can simultaneously observe a variety of fluorescently labeled molecules or organelles, providing a reliable means for studying biomolecule co-localization and interaction. In terms of dynamic observation, the time resolution of the technique is sufficient to capture rapidly occurring physiological processes in living cells, such as calcium ion fluctuation or vesicle transport. It should be noted that in the biofilm where several kinds of bacteria coexist, there is interaction between different kinds of bacteria, which makes the biofilm formation mechanism more complex. Therefore, finding strain-specific dyes and applying them to biofilm morphology research has become an important problem to be solved[5]. Modern laser confocal systems are usually equipped with high sensitivity detectors, which can detect weak fluorescence signals, greatly expanding the scope of its application in the study of low expression biological samples. These technological advantages make them indispensable and important tools for modern cell biology, developmental biology and nanomaterial research.

1.3 Overview of transmission electron microscope (TEM)

1.3.1TEM introduction to TEM

Transmission Electron Microscope (TEM) is a microanalytical technique that

utilizes a high-energy electron beam to penetrate through a sample and form a high-resolution image, with the imaging principle based on the interaction of electrons and matter. Compared with optical microscopy, TEM uses an electron beam with a very short wavelength as the illumination source, which breaks the optical diffraction limit and enables submicron-resolution ultrastructural observation. It is widely used in the fields of material science, nanotechnology, and life science. In the study of biological samples, TEM can clearly display the fine structures of organelles, such as ultrastructural features as mitochondrial crista and ribosomal distribution. In the aspect of material characterization, it can be used to analyze crystal defects, interface structure and nanoparticle morphology. This technique typically involves preparing the sample into ultra-thin sections (50-100 nm) and may involve special handling such as negative staining, freeze-fixing or metal projection to improve contrast[4]. Modern TEM systems are often equipped with energy dispersive spectroscopy (EDS) and electron energy loss spectroscopy (EELS) to obtain morphological information while analyzing the elemental composition and chemical state. TEM has extremely high spatial resolution, but its sample preparation is complex and the equipment cost is high. Besides, it requires certain conductivity and electron beam irradiation resistance of the samples. With the development of aberration correction technology and frozen electron microscopy, transmission electron microscopy has shown more powerful application potential in atomic-scale imaging and structural analysis of biological macromolecules.

1.3.2 Advantages of TEM

The most outstanding advantage of the transmission electron microscope (TEM) is its extremely high resolution. Thanks to the extremely short de Broglie wavelength of the electron beam, it can achieve the imaging ability in the sub-angstrom level (0.1 nm level), which far exceeds the diffraction limit of the optical microscope. This makes TEM become a powerful tool for observing the atomic arrangement of materials and the structure of biological macromolecules. This technique can not only provide the two-dimensional morphology information of samples, but also obtain the key material

science parameters such as crystal structure, lattice constant and orientation through the electronic diffraction pattern, thus providing direct evidence for crystal defect analysis and phase transformation research. Modern TEM equipped with EDS and EELS has further expanded its functions to realize in-situ analysis of chemical composition and electronic structure on the nanometer or even atomic scale. For biological samples, high-resolution TEM can clearly analyze the fine features of cell ultrastructure, such as nuclear pore complex and virus particles. The development of cryo-TEM makes it possible to observe biological macromolecules in a near-physiological state. In addition, through the three-dimensional reconstruction technology, TEM can also reconstruct the three-dimensional structure of samples, providing a unique perspective for understanding the three-dimensional defect distribution of materials or the spatial conformation of biological macromolecules. Despite the limitations of complex sample preparation and expensive equipment, TEM still has irreplaceable advantages in revealing the nature of the microstructure of materials, especially in the fields of nanomaterial characterization, semiconductor defect analysis and structural biology research, which plays a key role.

1.4 Research status at home and abroad

In recent years, the research on marine bacterial extracellular polysaccharide (EPS) in China and abroad has presented the trend of multi-dimensional in-depth exploration. Internationally, researchers have paid more and more attention to marine bacteria EPS derived from extreme environments (such as deep-sea hydrothermal solution and polar glacier). By using advanced chromatography-mass spectrometry technology and nuclear magnetic resonance (NMR) and other means, a variety of polysaccharides with novel structural characteristics have been resolved, such as EPS containing rare sugar units (such as rhamnose and fucose) or special modifications (such as sulfation and acetylation). These structural characteristics are often closely related to its unique biological activities (such as antiviral and antioxidant). In the application of microscopy, the introduction of cryo-EM and atomic force microscopy (AFM) enabled researchers to observe the supramolecular assembly morphology of

EPS in a near-physiological state, revealing the dynamic formation process of nano-sized fiber network or micelle-like structure. However, laser confocal microscopy (CLSM) combined with fluorescence labeling technology was widely used to in-situ study the spatial distribution of EPS in biofilm and its interaction with microbial communities. The domestic research teams have made significant progress in the research on marine bacterial EPS in the South China Sea, the East China Sea and other seas. They not only found a variety of polysaccharides with immunoregulatory and heavy metal adsorption functions, but also characterized the micro-morphological characteristics of EPS, such as porous network or granular structure, by using transmission electron microscopy (TEM) and scanning electron microscopy (SEM) systems, and initially established the correlation model between polysaccharide yield and culture conditions. However, there are still some challenges in the current research, for example, the understanding of the structure-activity relationship of EPS is not deep enough, the advanced structure analysis technology of polysaccharides is still limited, and the systematic research on the microstructure differences and biological significance of EPS from different strains is relatively lack. Future research is expected to further reveal the structural diversity of marine bacterial EPS and its potential in ecological adaptation and biotechnology application by integrating multi-component analysis, high-resolution micro-imaging and artificial intelligence prediction.

1.5 Research purpose and significance

This study was aimed at exploring the structural characteristics of exopolysaccharides from four marine bacteria. In the known studies, researchers mostly use traditional chemical and spectroscopy methods to explore the structure of exopolysaccharides and characterize the structural characteristics of exopolysaccharides. In this study, the relationship between the growth characteristics of different strains and EPS yield was analyzed by measuring the growth curve and polysaccharide content, and the high-yielding strain was screened. Four strains of bacteria with the capability of producing extracellular polysaccharide were tested by using transmission electron microscope and laser confocal microscope respectively:

Pseudoalteromonas agariverans HAO 2018 (p.A. HAO 2018; Hao2018）、*Bacillus velezensis* Hao 2022 (B.v. Hao2022；Hao2022）、Meta*Bacillus halosaccharovorans* Hao 2023 (M.h. Hao2023； Hao2023）、Staphylococcus pseudoxylosus Hao 2024 (S.p. Hao2024；So as to understand the different morphological characteristics of the four marine bacteria at different growth stages and the distribution of the exopolysaccharides secreted by the bacteria.

Conclusions to chapter 1

Multi-scale observation on the structural characteristics of four marine bacteria EPS will not only help to clarify the structure-activity relationship of EPS, but also provide a theoretical basis for the development of new bioactive materials. In addition, the correlation between the growth characteristics of the strain and the polysaccharide yield was analyzed, which provided reference for optimizing the fermentation process of EPS and had important application value. It has long been shown that marine microorganisms may be the true producers of natural active substances in their hosts[15]. This study not only expanded the utilization potential of marine microbial resources, but also provided a new perspective for in-depth understanding of the ecological function of EPS in the marine environment.

CHAPTER 2

OBJECT, PURPOSE AND METHODS OF THE STUDY

Marine bacteria have demonstrated significant diversity in metabolic pathways and product synthesis due to their unique living environment (such as high salt, low temperature, and high pressure). In particular, the synthetic ability of extracellular polysaccharide (EPS) has broad application potential in the fields of medicine, food, and environmental repair[7]. However, the growth characteristics and polysaccharide yield of different strains were significantly affected by the culture conditions (such as temperature, pH, and carbon source), and the internal regulatory mechanism was not fully elucidated[11].

In this study, four marine bacteria were selected and the correlation between growth kinetics and polysaccharide synthesis efficiency was systematically analyzed to reveal the correlation between strain growth and product synthesis, which laid a theoretical foundation for the industrial application of marine microbial resources.

2.1 Experimental materials, main instruments and equipment

Test strains and medium composition

Experimental strains: Hao 2018, Hao 2022, Hao 2023, and Hao 2024.

Sea salt fermentation medium: 45g/L glucose, 2.5g/L yeast extract, 35g/L sea salt, and 1000 mL deionized water at pH 8.0–9.0.

Experimental reagent (Table 2.1).

Table 2.1

Experimental reagents and manufacturers

Reagent	Specifications	Manufacturer
sea salt	AR	Shandong yousuo chemical technology co., ltd
yeast extract	AR	Dezhou runxin chemical experimental instrument co., ltd
peptone	AR	Dezhou runxin chemical experimental instrument co., ltd
sodium hydroxide	AR	National Pharmaceutical Group Chemical

Reagent	Specifications	Manufacturer
		Reagent Co., Ltd
95% ethanol	AR	Shandong deyan chemical co., ltd
98% concentrated sulfuric acid	AR	Yantai Yuandong Fine Chemical Co., Ltd.
normal saline	AR	Shandong yousuo chemical technology co., ltd

Strain

The strains used in this experiment were: *Pseudoalteromonas agarivers* HAO 2018, *Bacillus velezensis* Hao 2022, Meta-*Bacillus halosaccharovorans* HAO 2023, and *Staphylococcus pseudodoxorus* HAO 2024.

The strain sources for this experiment are shown in the following table 2.2.

Table 2.2

Strain used in this chap

Bacterial strain	Source
Pseudoalteromonas agarivorans Hao 2018 (*P.a. Hao2018；Hao2018*)	Laboratory preservation
Bacillus velezensis Hao 2022 (*B.v. Hao2022；Hao2022*)	Laboratory preservation
MetaBacillus halosaccharovorans Hao 2023 (*M.h. Hao2023；Hao2023*)	Laboratory preservation
Staphylococcus pseudoxylosus Hao 2024 (*S.p. Hao2024；Hao2024*)	Laboratory preservation

Main instruments and equipment (Table 2.3).

Table 2.3

Experimental equipment and manufacturers

Instrument name	Manufacturer
Ultraviolet visible light spectrophotometer	Shanghai yuanxi instrument co., ltd
Refrigerated refrigerator	Changhong Meiling Co., Ltd.
Electronic balance	Olaibo electronics co ., ltd
Ph meter	Bang billion precision instrument co., LTD
High pressure steam sterilizer	Alaibao Medical Technology Co., Ltd.
Constant temperature oscillation incubator	Shanghai Shanzhi Instruments Co., Ltd.
Magnetic stirrer	Gongyi city yingyu hongyuan instrument

Instrument name	Manufacturer
	factory
Superclean bench	Shanghai gonai purification equipment co ., ltd
high-speed freezing centrifuge	Eppendorf corp
Laser confocal microscope	Nikon Instruments (China) Co., Ltd
Transmission electron microscope	Thermo Fisher Scientific shier technology (China) co ., ltd
Pipette	Eppendorf corp

2.2 Experimental methods

2.2.1 Growth curve drawing

Bacterial growth curve refers to a curve drawn by inoculating a small amount of single-cell microorganisms into a liquid culture medium and culturing under appropriate conditions, taking out the sample on time, and measuring the number of cells in the sample, taking the logarithm of the number of cells as the vertical coordinate and the culturing time as the horizontal coordinate, which is called the bacterial growth curve. The growth curve of bacteria reflects the growth law of microorganisms under certain culture conditions[10]. We explored the growth law of four marine bacteria by drawing their growth curves. So as to determine the characteristics of different special structures at different growth stages of the bacteria. There are many methods for measuring the number of microorganisms, which can be selected according to conditions and needs. In this experiment, the turbidity method was used for determination. Under certain conditions, the microbial concentration was in direct proportion to the optical density. Therefore, the optical density (OD value) of the bacterial liquid could be measured by a spectrophotometer, and then the growth curve could be drawn by plotting the measured OD value with the culture time.

The specific procedures are as follows.

(1) Activation: The bacterial liquid was inoculated into LB medium and cultured in a 37 C shaking table for 12 hours for later use.

(2) Labeling: Seventy-six pieces of fresh sea salt medium were taken and the culture time was marked with a marker pen, namely, 0 h, 2 h, 4 h, 6 h, 8 h, 10 h, 12 h, 14

h, 16 h, 18 h, 20 h, 22 h, 24 h, 26h, 28h, 30h, 32h, 34h and 36 h.

(3) Inoculation: the activated strains were inoculated into the labeled medium with the inoculation amount of 10%, and cultured in a shaking table at 37^{o} C.

(4) Detection: The culture medium was sequentially taken out according to the labeling time, and the absorbance of the bacterial solution was measured at a wavelength of 600 nm by using an ultraviolet spectrophotometer.

(5) Draw the curve: According to the measured data, the growth curve of bacteria was drawn on Graphpad Pism software.

2.2.2 Determination of extracellular polysaccharide content

UV-Vis spectrum is one of the commonly used instrumental analysis methods in polysaccharide structure study. For example, phenol-sulfuric acid method and anthrone-sulfuric acid method are used to determine the polysaccharide content, while carbazole-sulfuric acid method is used to determine the uronic acid content. The elution curve of polysaccharide is drawn by phenol-sulfuric acid method during column chromatography[13].

2.2.2.1 Determination of glucose standard curve by phenol-sulfuric acid method

Weigh 20 mg of glucose, dissolve in distilled water, and adjust the volume to a 500-mL volumetric flask. Absorb 0 mL, 0.4 mL, 0.6 mL, 0.8 mL, 1.0 mL, 1.2 mL, 1.4 mL, 1.6 mL, and 1.8 mL of glucose solution, and adjust the volume to 2 mL with distilled water. To the solution was added 1 mL6% of 6% phenol and 5 mL of concentrated sulfuric acid, shaken homogeneously, and placed in a 30 C water bath for reaction for 20 minutes with the absorbance measured at 490 nm. The standard curve was plotted with the mass of glucose as the horizon coordinate and the absorbance at 490 nm as the vertical coordinate.

2.2.2.2 Determination of extracellular polysaccharide yield of strain

Centrifuging 1 mL of fermentation liquid (5000 rpm for 20 min) to remove thalli,

adding 3 times of volume of 95% ethanol into the supernatant, precipitating in a refrigerator at 4 deg c overnight, (8000 rpm for 10 min), centrifuging to collect precipitate, adding 5 mL of distilled water to dissolve, extracting 1 mL from the solution, adding 1 mL of distilled water to dilute to 10 times, adding 1 mL of 6% phenol, 5 mL of 98% concentrated sulfuric acid, After sufficient oscillation, the mixture was allowed to react for 20 minutes, and the absorbance was measured at 490 nm, and then the polysaccharide content was converted according to the glucose standard curve measured by 2.2.2.1.

2.2.3 Laser scanning confocal microscope (CLSM)

Laser scanning confocal microscope (CLSM) combined with fluorescence labeling technology is a powerful tool for studying the spatial distribution and interaction of microorganisms and polysaccharides. In this chapter, FITC-ConA (green fluorescence) was used to label polysaccharides, and DAPI (red fluorescence) was used to label bacterial DNA.

The specific procedures are as follows.

(1) Activation: The bacterial liquid was inoculated into LB medium and cultured in a 37 C shaking table for 12 hours for later use.

(2) Labeling: 120 pieces of fresh sea salt medium were taken and the culture time was marked with a marker pen, namely, 4 h, 22 h and 36 h.

(3) Inoculation: the activated strains were inoculated into the labeled medium with the inoculation amount of 10%, and cultured in a shaking table at 37 C.

(4) Sample preparation: the culture medium was taken out in sequence according to the labeling time, and 10 samples of culture medium for each strain at each time point were taken out and divided into Group A, Group B and Group C (for electron microscopy, live cell staining and dead cell staining, respectively), centrifuged at 2000 rpm for 10 minutes at 4 C, the supernatant was discarded, and 1 mL of PBS was added for precipitation and repeated washing for 2–3 times. Group A was fixed overnight at 4 C with 2.5% glutaraldehyde (current formulation), while group C was fixed with 4% paraformaldehyde (reacting for 20–30 minutes at normal temperature) and centrifuged

at 2000 rpm for 10 minutes, PBS was performed for two times to leave the precipitate, and then groups B and C were stained: 500μL FITC-ConA was added to stain the precipitate, and the precipitate was centrifuged at 2000 rpm after reacting in the dark for 30 minutes. After being washed with PBS, 500μL PI(DNA) was added for staining. After reacting for 30 minutes in the dark, the precipitate was left after centrifugation. After being washed for 1–2 times with PBS, 200μLPBS was added and the thalli were re-suspended. Then 15μL bacteria liquid was taken and dropped into the center of the glass slide and covered with a cover glass, and the plate was naturally dried at room temperature.

(5) Microscopic observation: Two-channel acquisition was adopted. The red channel was acquired first and then the green channel was acquired. Afterwards, image stacking was performed for result analysis. The results obtained with 20-fold mirror and 100-fold mirror (oil lens) showed significant differences in resolution, field of view and imaging details.

CHAPTER 3
EXPERIMENTAL PART

3.1 Determination of growth curve

3.1.1 Growth curve of *Pseudoalteromonas agarivers* HAO 2018

The samples were cultured at 25 C and sampled at different time periods. The OD600 value of Hao 2018 bacterial solution was continuously measured by the ultraviolet spectrophotometer within 36 h. According to the measured OD600 value of bacterial liquid, the growth curve of strain Hao 2018 was drawn using Graphpad Pism software (Fig. 3.1).

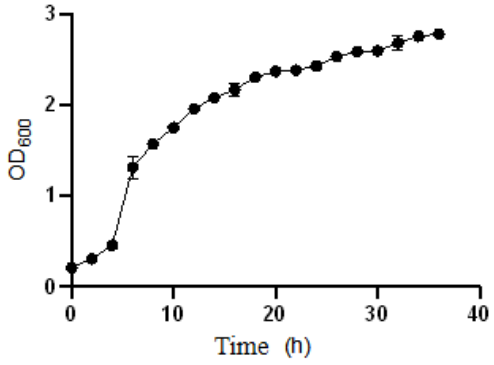

Figure 3.1 – Growth curve of strain Hao 2018 at 25 C

Under the condition of 25^{o}C, the strain Hao 2018 began to enter the exponential growth period of rapid growth at about 4 h, and the growth rate slowed down at about 18 h and began to enter the growth stability period.

3.1.2 Growth curve of *Bacillus velezensis* HAO2022

The samples were cultured at 25 ^{o}C and sampled at different time points. The OD600 value of Hao 2022 bacterial solution was continuously measured by ultraviolet spectrophotometer within 36 h. According to the measured OD600 value of bacterial liquid, the growth curve of strain Hao 2022 was drawn by Graphpad Pism software (Fig. 3.2). Under the condition of 25 ^{o}C, the strain Hao 2022 begins to enter the exponential growth period of rapid growth at about 2 h, and slows down at about 12 h, and begins to enter the growth stability period.

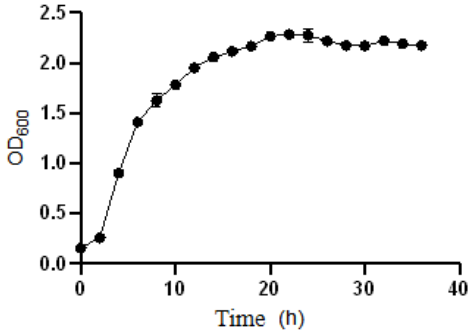

Figure 3.2 – Growth curve of strain Hao 2022 at 25 °C

3.1.3 Growth curve of Meta- *Bacillus halaccharovorans* HAO 2023

The samples were cultured at 25 C and sampled at different time points. The OD600 value of Hao 2023 bacterial solution was continuously measured by ultraviolet spectrophotometer within 36 h. According to the measured OD600 value of bacterial solution, the growth curve of strain Hao 2023 was drawn using Graphpad Pism software (Fig. 3.3). Under the condition of 25 °C, the strain Hao 2023 began to enter the exponential growth period of rapid growth at about 2 h, and the growth rate slowed down at about 24h and began to enter the growth stability period. At about 26 h, the concentration of bacterial liquid began to decrease slowly and the surface bacteria began to enter the decline phase.

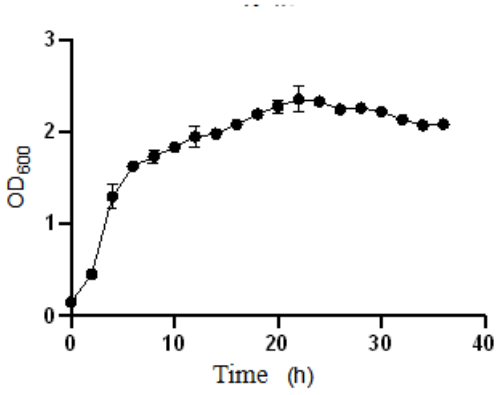

Figure 3.3 – Growth curve of strain Hao 2023 at 25 °C

3.1.4 Growth curve of *Staphylococcus pseudomonas* HAO2024

The samples were cultured at 25 °C and sampled at different time points. The

OD600 value of Hao 2024 bacterial solution was continuously measured by ultraviolet spectrophotometer within 36 h. According to the measured OD600 value of bacterial liquid, the growth curve of strain Hao 2024 was drawn by Graphpad Pism software (Fig. 3.4). The strain Hao 2024 begins to enter an exponential growth period of rapid growth at about 2 h under the condition of 25 ^{o}C, and slows down at about 18h and begins to enter a growth stable period.

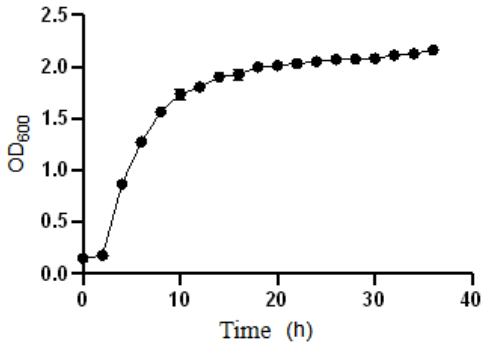

Figure 3.4 – Growth curve of strain Hao 2024 at 25 ^{o}C

3.2 Determination of extracellular polysaccharide content

3.2.1 Rawing of standard curve of phenol-sulfuric acid method

After the determination according to the method of 2.2.2.1, with glucose mass as the abscissa, absorbance at 490 nm as the ordinate to draw the standard curve (Fig. 3.5). The obtained equation was y = 0.0049x+0.0047, and R^2 = 0.9982, with good fitting degree.

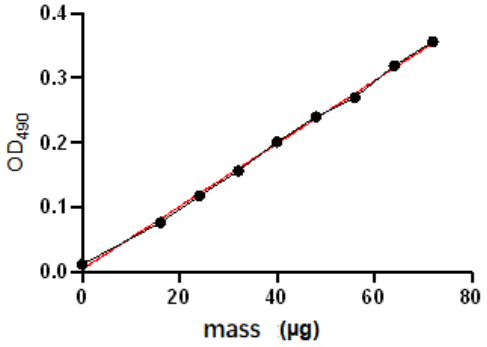

Figure 3.5 – Glucose standard curve

3.3.2 Yield of extracellular polysaccharides from *Pseudoalteromonas agarivers* HAO 2018

The extracellular polysaccharide content of the bacterial liquid was determined according to the method of 2.2.2.2, and the extracellular polysaccharide content was converted according to the standard curve obtained by 2.2.2.1. As shown in Fig. 3.6, the sugar production of this strain in the stable stage of growth was about 0.3 g/L.

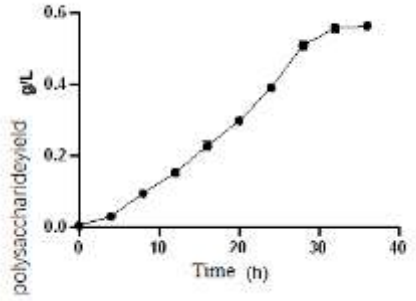

Figure – 3.6 Standard curve of strain Hao 2018

3.2.3 Extracellular polysaccharide production of *BACILLUS VELEZENSIS* HAO2022

The extracellular polysaccharide content of the bacterial liquid was determined according to the method of 2.2.2.2, and the extracellular polysaccharide content was converted according to the standard curve obtained by 2.2.2.1. As shown in Fig. 3.7, the sugar production of this strain in the stable stage of growth was about 0.18 g/L.

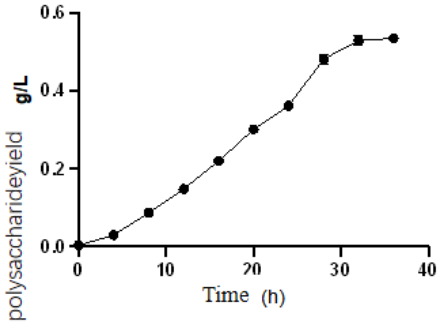

Figure 3.7 – Standard curve of strain Hao 2022

3.2.4 Extracellular polysaccharide yield of Meta-*Bacillus halaccharovorans* HAO 2023

The extracellular polysaccharide content of the bacterial liquid was determined according to the method of 2.2.2.2, and the extracellular polysaccharide content was converted according to the standard curve obtained by 2.2.2.1. As shown in Fig. 3.8, the sugar production of this strain in the stable stage of growth was about 0.4 g/L.

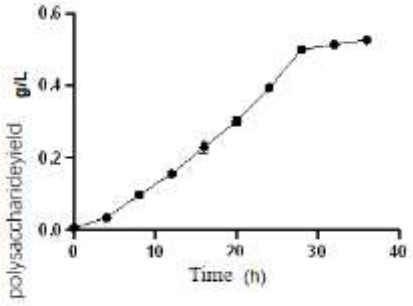

Figure – 3.8 Standard curve of strain Hao 2023

3.2.5 Exopolysaccharide yield of *Staphylococcus pseudoxylosus* HAO 2024

The extracellular polysaccharide content of the bacterial liquid was determined according to the method of 2.2.2.2, and the extracellular polysaccharide content was converted according to the standard curve obtained by 2.2.2.1. As shown in Fig. 2.9, the sugar production of this strain in the stable stage of growth was about 0.25 g/L.

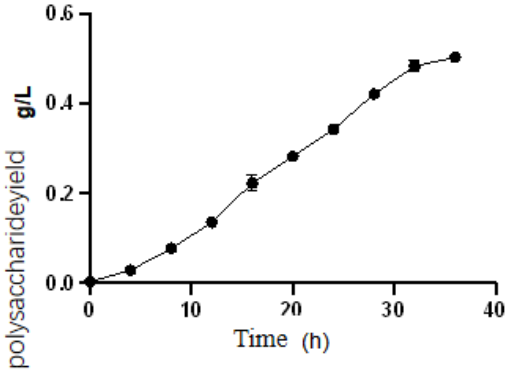

Figure 3.9 – Standard curve of strain Hao 2024

This chapter focuses on the growth characteristics and extracellular polysaccharide production of four marine bacteria. The aim of this study is to investigate the growth characteristics of four bacteria with significant adaptability to the marine environment and evaluate their extracellular polysaccharide production, providing potential bacterial resources for the further development of new microbial drugs and biological products. These four marine bacteria were isolated from [specific sea area and environment, e.g., seawater samples from a certain area of the South China Sea] and identified to [specific taxonomic status, e.g., genus and species name, or only to the genus level] through methods such as morphological observation, physiological and biochemical characteristic tests, and 16S rRNA gene sequence analysis. To study their growth characteristics, we first determined their OD600 values at different culture time points and recorded the data. By plotting growth curves, we can intuitively observe the growth patterns of these four marine bacteria, including the lag phase, logarithmic phase, stationary phase, and decline phase. In addition, we will further analyze the growth curves, such as comparing the differences in growth rate, maximum biomass, and growth cycle between different strains. Next, we used the phenol-sulfuric acid method to determine the extracellular polysaccharide production of these four marine bacteria. The phenol-sulfuric acid method is a commonly used method for polysaccharide quantification. Its principle is that polysaccharides are hydrolyzed into monosaccharides under the action of concentrated sulfuric acid, and the monosaccharides are rapidly dehydrated to form furfural derivatives, which then condense with phenol to form an orange compound. The absorbance value of this compound at 490 nm is directly proportional to the polysaccharide content. By measuring the absorbance value and combining it with the standard curve, we can calculate the yield of extracellular polysaccharides. Ultimately, we will comprehensively evaluate the development and utilization value of these four marine bacteria based on the results of the growth curves and extracellular polysaccharide production, and provide a theoretical basis for the further development and utilization of marine microbial resources.

The functional properties of microbial extracellular polysaccharide (EPS) are closely related to its spatial distribution and microstructure. However, it is difficult to clearly observe the stereo-conformation of polysaccharide-bacteria interaction with the traditional optical microscope due to the limited resolution. Laser scanning confocal microscope (CLSM) can visually analyze the attachment morphology, three-dimensional network structure of polysaccharides on the bacterial surface and their dynamic correlation with bacterial growth by virtue of its high-resolution tomography and multi-fluorescence channel synchronous imaging capabilities, providing key visual evidence for revealing the polysaccharide synthesis mechanism.

3.3. Microscopic observation and analysis

3.3.1 Observation of *Pseudoalteromonas agarivers* HAO 2018

3.3.1.1 Observation on strain HAO 2018 4H

As shown in Fig. 3.10, the red fluorescence signal and green fluorescence signal were distributed sporadically, indicating the existence and diffusion pattern of polysaccharides on the cell surface or extracellular matrix, and the small number of yellow overlapping regions, which might be attributed to the small production of extracellular polysaccharides at 4 h.

Note: This plate shows four sets of fluorescence microscope images (labeled A-D) obtained in a characterization study of marine bacterial extracellular polysaccharide (EPS):

Figure A: Open-field micrograph showing morphological characteristics of primitive cells from a bacterial sample.

Fig. B: The falling fluorescence image obtained with red fluorescent nucleic acid dye (PI) showed a punctiform red fluorescence signal, corresponding to the localization and distribution of bacterial genomic DNA.

Figure C: Visualization image of EPS labeled with green fluorescence by FITC, showing typical polysaccharide-related fluorescence distribution pattern.

Figure D: composite fluorescence micrograph showing:-red channel: DNA signal

(same as figure b)-green channel: EPS signal (same as figure c)-yellow area: signal co-localization area (RGB overlay), indicating the spatial association of EPS with bacterial cells

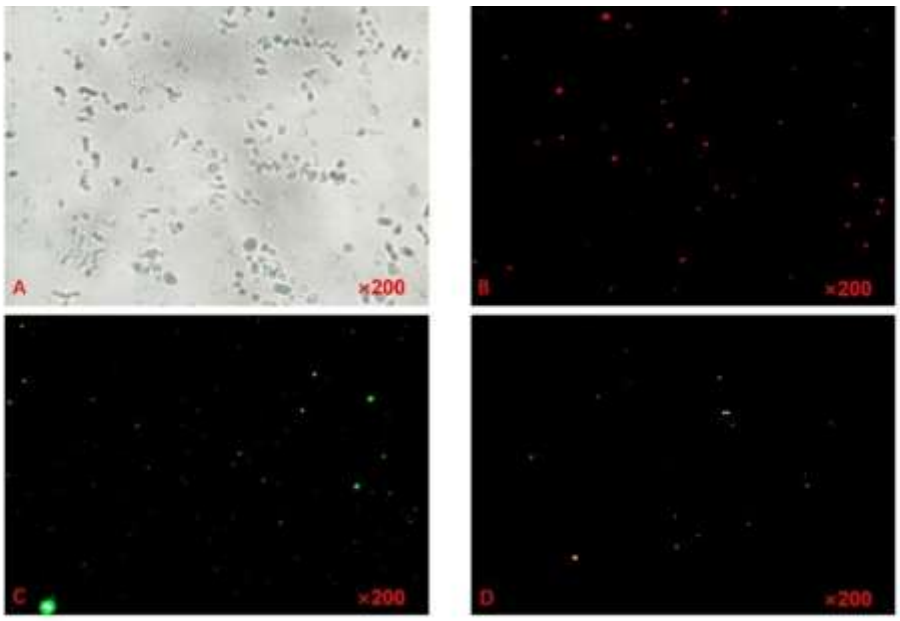

Figure 3.10 – Microscopic result of 4h 20-fold fixation of strain Hao 2018

As shown in Fig. 3.11, the morphology of Hao 2018 was rod-shaped, and the red fluorescence signal and green fluorescence signal were distributed sporadically, indicating the existence and diffusion pattern of polysaccharides on the cell surface or extracellular matrix. The yellow overlapping area was relatively obvious, indicating that there was a certain degree of co-localization between bacterial surface polysaccharides and cell surface markers.

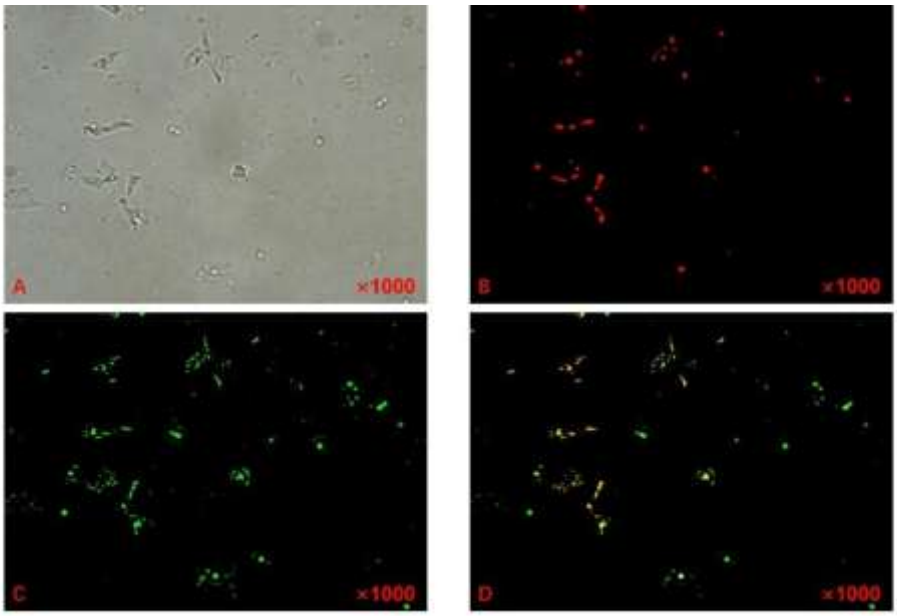

Figure 3.11 – Microscopic results of 4h 100-fold fixation of strain Hao 2018

As shown in Fig. 3.12 the red fluorescence signal and green fluorescence signal were more diffuse and dynamic in distribution, indicating the existence and diffusion pattern of polysaccharides on the cell surface or extracellular matrix, and less yellow overlapping area, which might be due to the small yield of 4h exopolysaccharide, unfixed sample and limited permeability of dye.

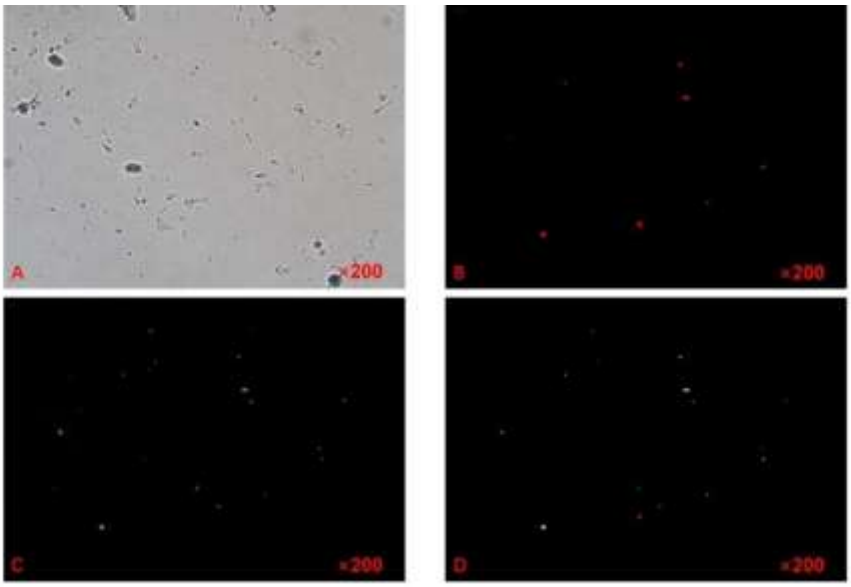

Fiure 3.12 – Microscopic result of strain Hao 2018 without fixation for 4 h and 20 times

As shown in Fig. 3.13, the red fluorescence signal and green fluorescence signal were more diffuse and dynamic in distribution. The real-time secretion trace of EPS could be seen, revealing the existence and diffusion pattern of polysaccharides on the cell surface or extracellular matrix, and the few yellow overlapping regions, which might be due to the fact that the yield of exopolysaccharides was small and the samples were not fixed at 4h, and the permeability of dyes was limited.

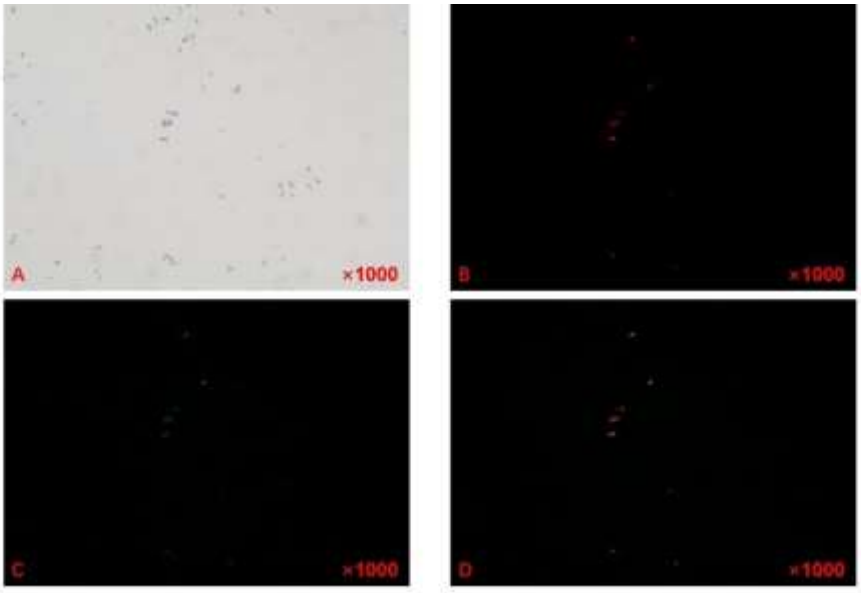

Figure 3.13 – Microscopic results of strain Hao 2018 without fixation for 4 h and 100 times

3.3.1.2 Observation on strain HAO 2018 22H

As shown in Fig. 3.14, the red fluorescence signal was dense, and the green fluorescence signal was scarce, indicating the existence and diffusion mode of polysaccharides on the cell surface or extracellular matrix, and the yellow overlapping area was scarce, indicating that polysaccharides might mostly exist in the free state and the yield of bacterial polysaccharides in the logarithmic phase was low.

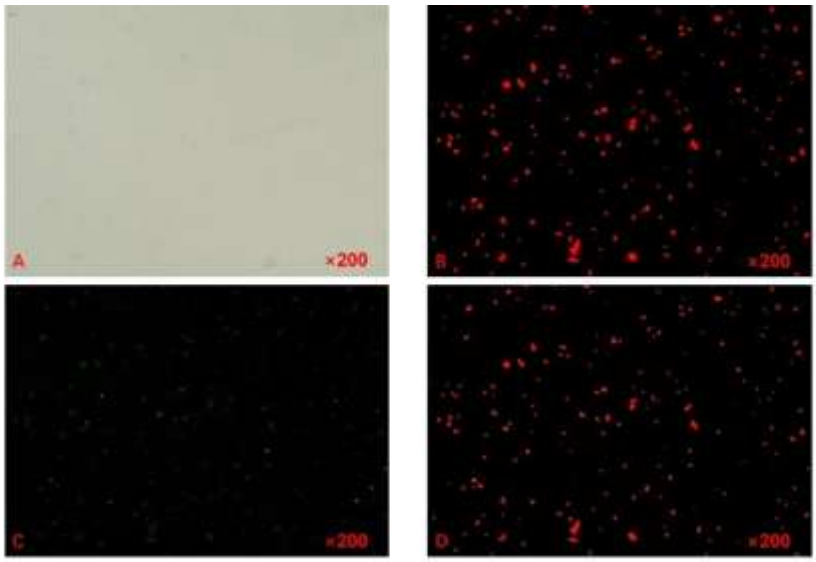

Figure 3.14 – 22h 20-fold microscopic results of bacterial strain Hao 2018 fixation

As shown in Fig. 3.15, oil microscope observation showed a higher resolution, with concentrated red fluorescence signal and green fluorescence signal distribution, to know the existence and diffusion pattern of polysaccharides on the cell surface or extracellular matrix, and the yellow overlapping area was very obvious, indicating that there was a large degree of co-positioning between bacteria surface polysaccharides and cell surface markers, which to some extent reflected that bacteria wrapped themselves by EPS to form a protective matrix.

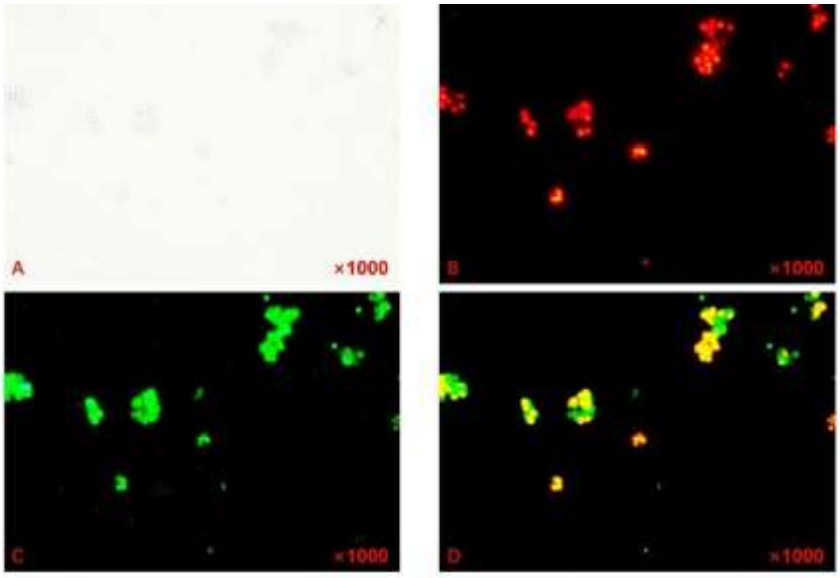

Figure 3.15 – Results of 22h 100fold endoscopy of strain Hao 2018 fixation

As shown in Fig. 3.16, the red fluorescence signal and green fluorescence signal were distributed sporadically, indicating the existence and diffusion pattern of polysaccharides on the cell surface or extracellular matrix. The yellow overlapping area was not obvious, which might be related to the unfixed bacterial sample.

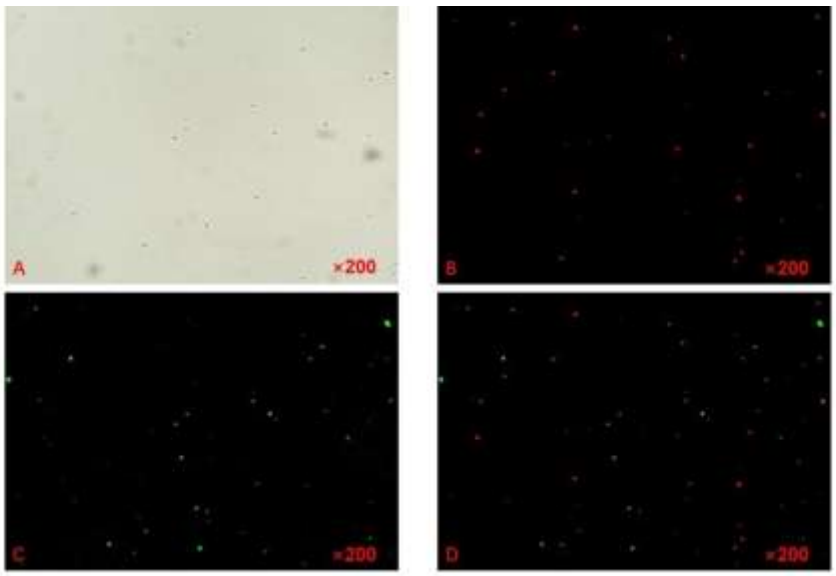

Figure 3.16 – Twenty-fold microscopic results of strain Hao 2018 without fixation for 22h 20

As shown in Fig. 3.17, the red fluorescence signal and the green fluorescence signal are very rare, and no yellow overlapping area is found, which may be due to bacterial death or metabolic stagnation, or the influence of microscope light source.

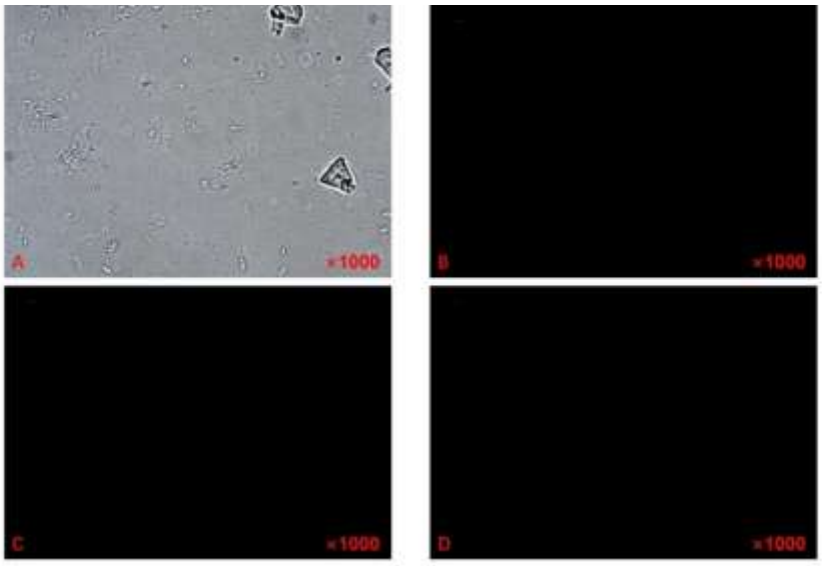

Figure 3.17 – Mirror result of 22h 100fold fixation of strain Hao 2018

3.3.1.3 Observation on strain HAO 2018 36H

As shown in Fig. 3.18, red fluorescence signal and green fluorescence signal were scarce, indicating the existence and diffusion mode of polysaccharides on the cell surface or extracellular matrix; the yellow overlapping area was scarce, indicating that polysaccharides might mostly exist in the free state and the yield of bacterial polysaccharides in the logarithmic phase was low.

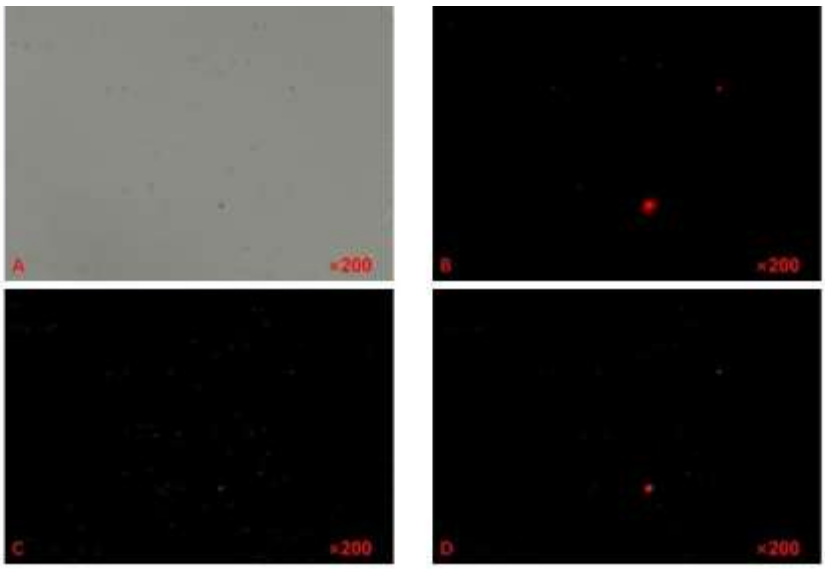

Figure 3.18 – Results of 36h 20-fold endoscopy of strain Hao 2018 fixation

As shown in Fig. 3.19, oil microscope observation showed a higher resolution. The distribution of red fluorescence signal and green fluorescence signal were relatively concentrated, and the yellow overlapping area was very obvious, indicating that there was a large degree of co-localization between bacterial surface polysaccharides and cell surface markers, which to a certain extent reflected that bacteria wrapped themselves by EPS to form a protective matrix.

As shown in Fig. 3.20, the red fluorescence signal was strong and widely distributed, the green fluorescence signal was relatively dispersed and the overall signal was weak, and the yellow overlapping area was not significant. It was possible that EPS might degrade because the bacterial sample was not fixed, the green dye was not completely penetrated, and the bacterial was in the decline phase.

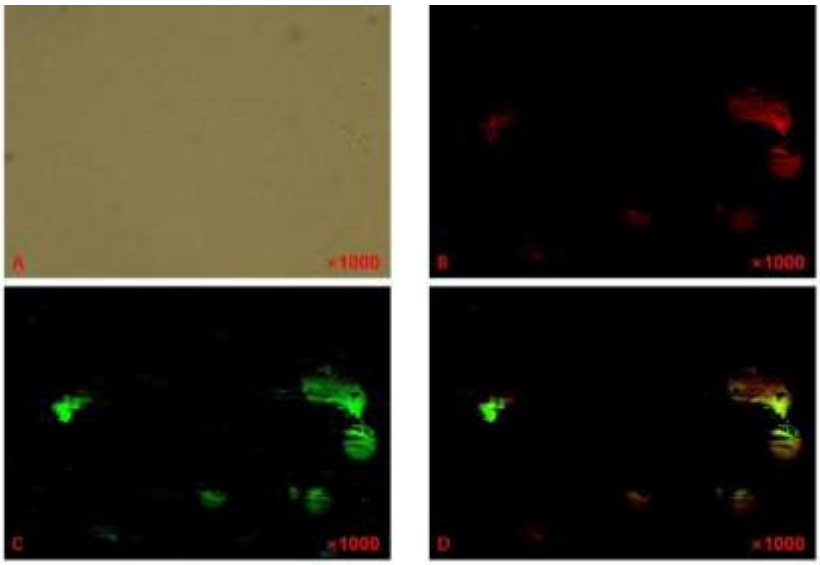

Figure 3.19 – Microscopic results of 36 h and 100 times fixation of strain Hao 2018

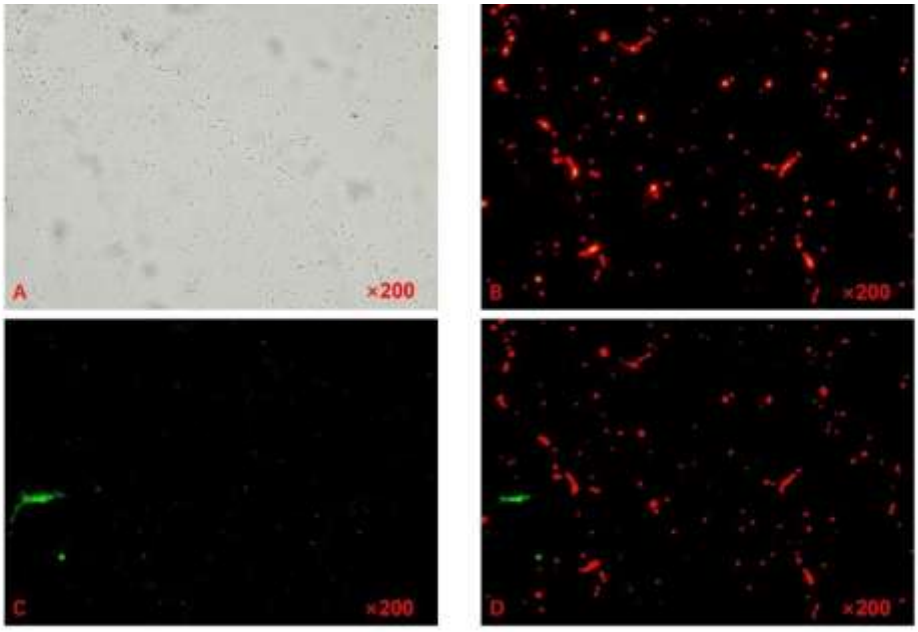

Figure 3.20 – Non-fixed 36h 20-fold microscopic result of strain Hao 2018

As shown in Fig. 3.21, the green fluorescence signal distribution and the red fluorescence signal distribution were relatively dispersed, but the yellow overlapping area was significant, indicating that there was a large degree of co-localization between bacterial surface polysaccharides and cell surface markers, which to some extent reflected that bacteria wrapped themselves by EPS to form a protective matrix.

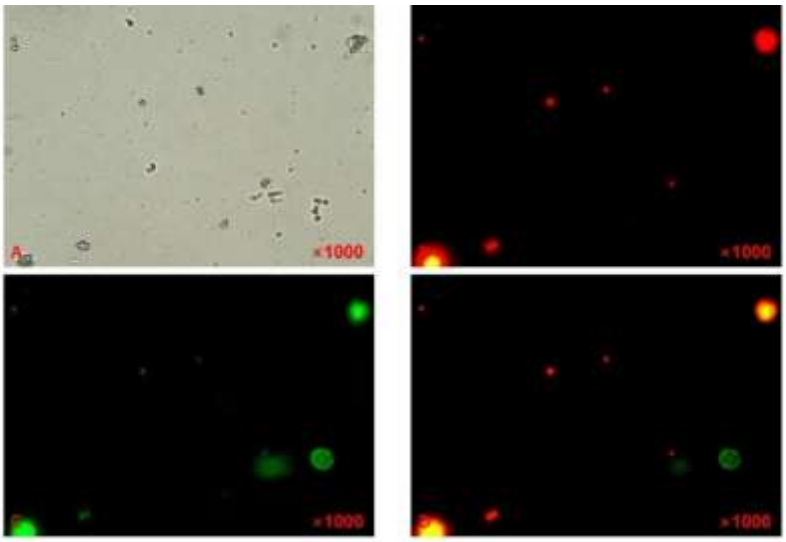

Figure 3.21 – Non-fixed 36h 100fold microscopic result of strain Hao 2018

3.4 Observation

3.4.1 *Bacillus velezensis* HAO 2022

3.4.1.1 Observation on strain HAO2024H

As shown in Fig. 3.22, the red fluorescence signal was densely distributed and there was a large number of them. The green fluorescence signal was widely distributed, and the yellow overlapping area was not significant. The reason might be that the green dye was quenched due to long-time illumination, the red dye was dominant, or the culture time of the strain was too short, and the polysaccharide yield was small.

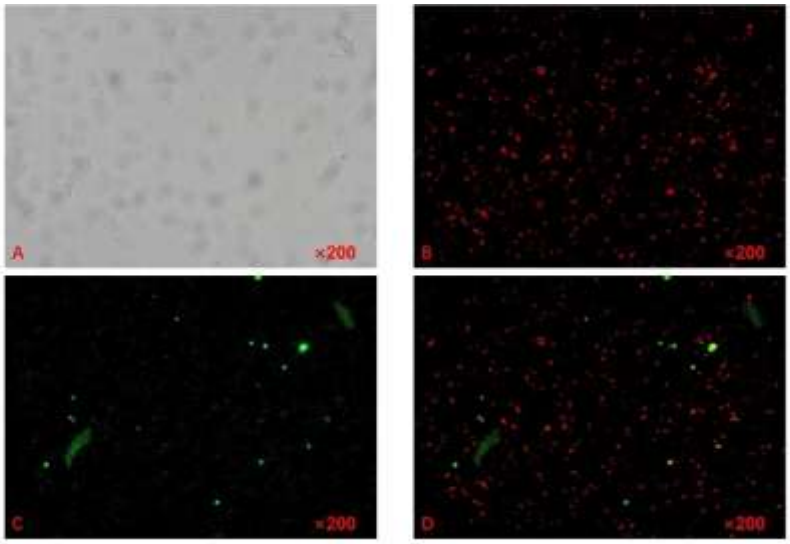

Figure 3.22 – Microscopic results of 4h 20-fold fixation of strain Hao 2022

As shown in Fig. 3.23, the bacterial strain was rod-shaped, and the green fluorescence signals were distributed intensively and in large numbers. The red fluorescence signals were distributed more dispersedly, and the yellow overlapping area was obvious, indicating that the extracellular polysaccharide of the bacterial strain was distributed intensively and the bacteria were in the stable phase (EPS) secretion exuberant. Excessive labeling and overexposure or excessive gain of the green channel due to excessive temperature could not be ruled out.

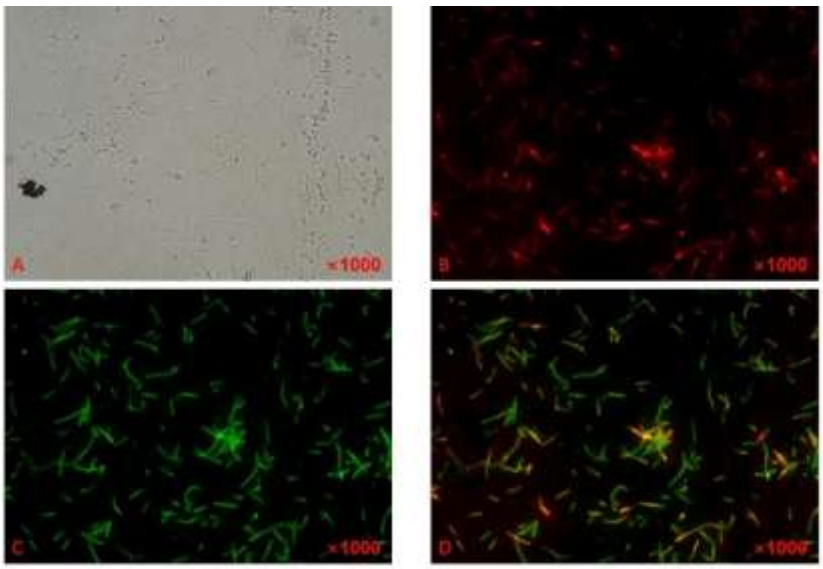

Figure 3.23 – Microscopic results of strain Hao 2022 fixed for 4 h and 100 times

As shown in Fig. 3.24, the red fluorescence signal and green fluorescence signal were distributed sporadically, indicating the existence and diffusion pattern of polysaccharides on the cell surface or extracellular matrix. The yellow overlapping area was not significant, which might be related to the unfixed bacterial sample (free EPS vulnerable to shearing force). It is not excluded that the EPS was distributed unevenly in the biofilm.

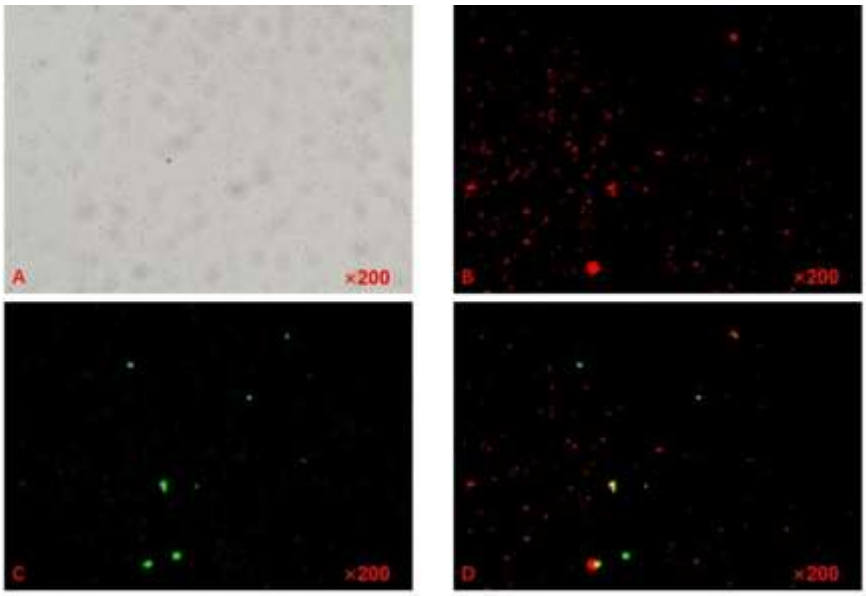

Figure 3.24 – Non-fixed 4h 20-fold microscopic results of strain Hao 2022

As shown in Fig. 3.25, it could be clearly seen that the bacterial strain was rod-shaped, the distribution of red fluorescence signal was fragmented, and the green fluorescence signal was weak, indicating the existence and diffusion pattern of polysaccharides on the cell surface or extracellular matrix. The yellow overlapping area was not significant, which might be related to the unfixed bacterial sample (free EPS vulnerable to shear stress). In addition, bacteria were in the logarithmic phase and preferred to proliferate rather than secrete EPS.

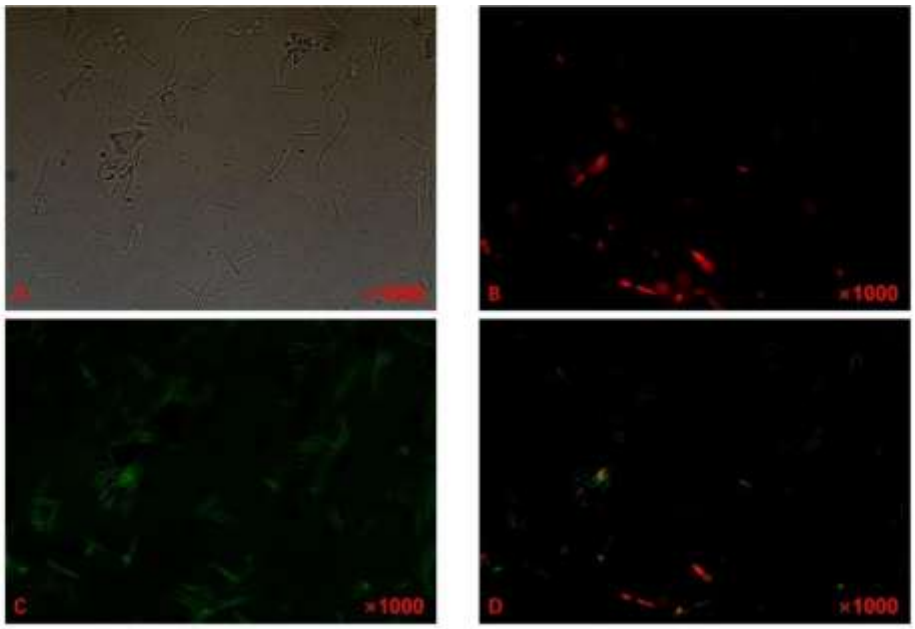

Figure 3.25 – Non-fixed 4h 100-fold microscopic results of strain Hao 2022

3.4.1.2 Observation on strain HAO 2022 22H

As shown in Fig. 3.26, the red fluorescence signal distribution was fragmented and the signal was weak, while the green fluorescence signal was strong, indicating the existence and diffusion pattern of polysaccharides on the cell surface or extracellular matrix. The yellow overlapping area was not significant. The strain was in the stable stage (the critical stage of biofilm formation), and the decline in the efficiency of red dye labeling could not be ruled out.

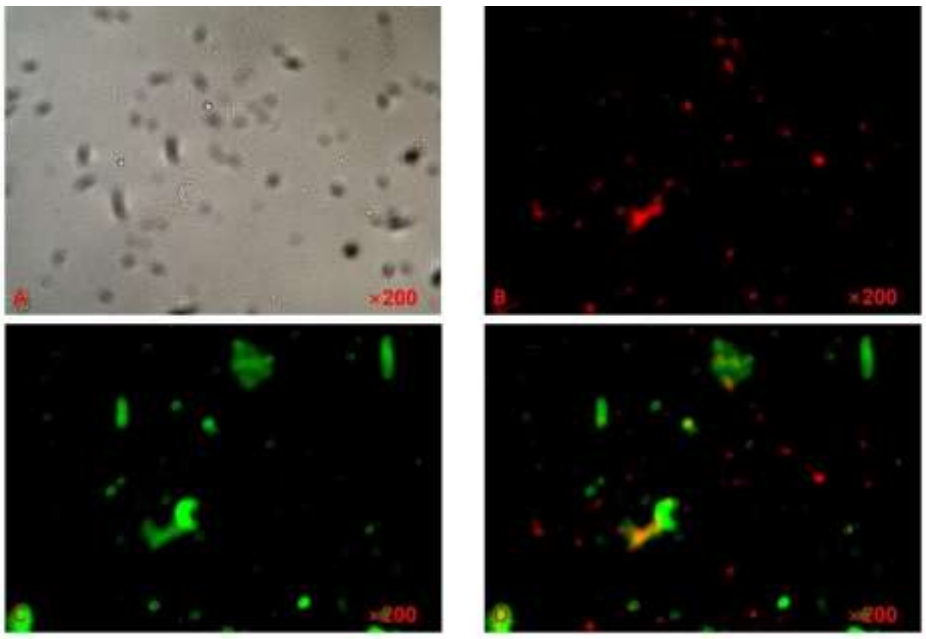

Figure 3.26 – 22h 20-fold microscopic results of bacterial strain Hao 2022 fixation

As shown in Fig. 3.27, oil microscope observation showed a higher resolution. It was clear that the bacterial strain was in the shape of a rod. The red fluorescence signal and green fluorescence signal were widely and densely distributed, and the yellow overlapping area was very obvious, indicating that there was a large degree of co-localization between bacterial surface polysaccharides and cell surface markers, which to some extent reflected that bacteria wrapped themselves by EPS to form a protective matrix. Moreover, the bacterial strain was in a stable stage, and EPS secretion was strong.

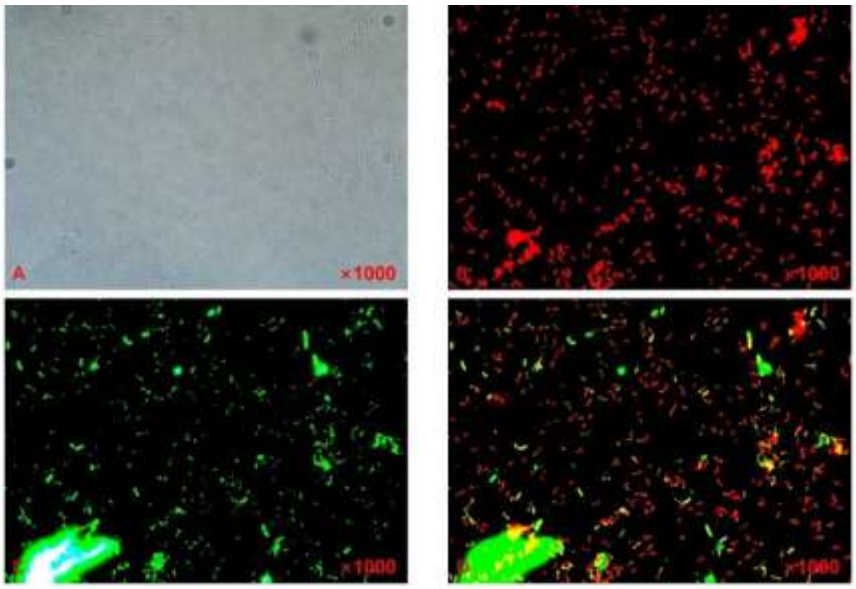

Figure 3.27 – Results of 22h 100fold endoscopy of strain Hao 2022 fixation

As shown in Fig. 3.28, the red fluorescence signal and the green fluorescence signal were very rare, and no yellow overlapping area was observed, probably due to the unfixed sample and incomplete dye penetration.

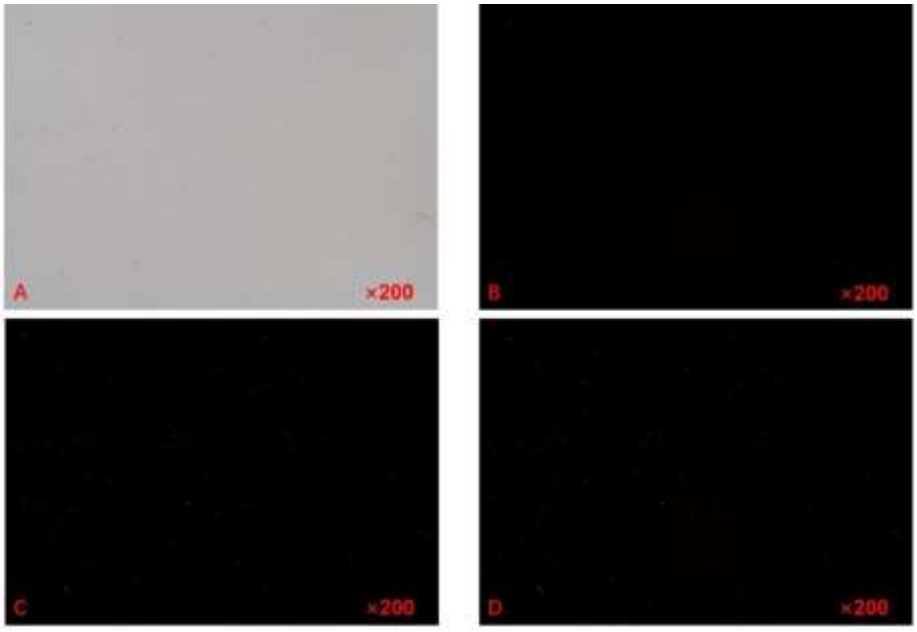

Figure 3.28 – Non-fixed 22h 20fold microscopic result of strain Hao 2022

As shown in Fig. 3.29, the red fluorescence signal and the green fluorescence signal were very rare, and no yellow overlapping area was observed, probably due to the unfixed sample and incomplete dye penetration.

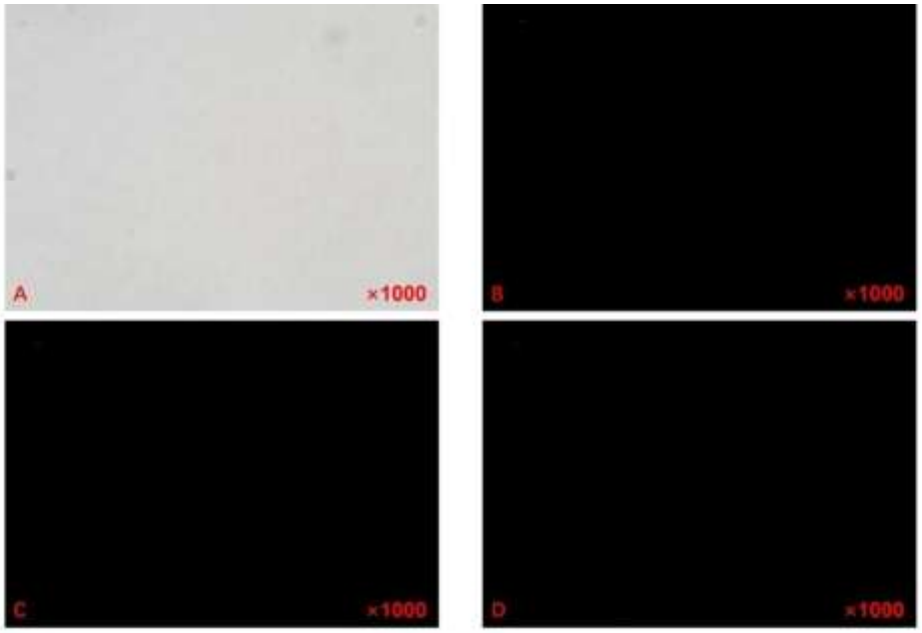

Figure 3.29 – Non-fixed 22h 100fold microscopic result of strain Hao 2022

3.4.1.3 Observation on strain HAO 2022 36H

As shown in Fig. 3.30, the red fluorescence signal was densely and uniformly distributed, with few green fluorescence signals and few yellow overlapping regions, which might be due to the degradation of EPS by bacteria in the decline phase.

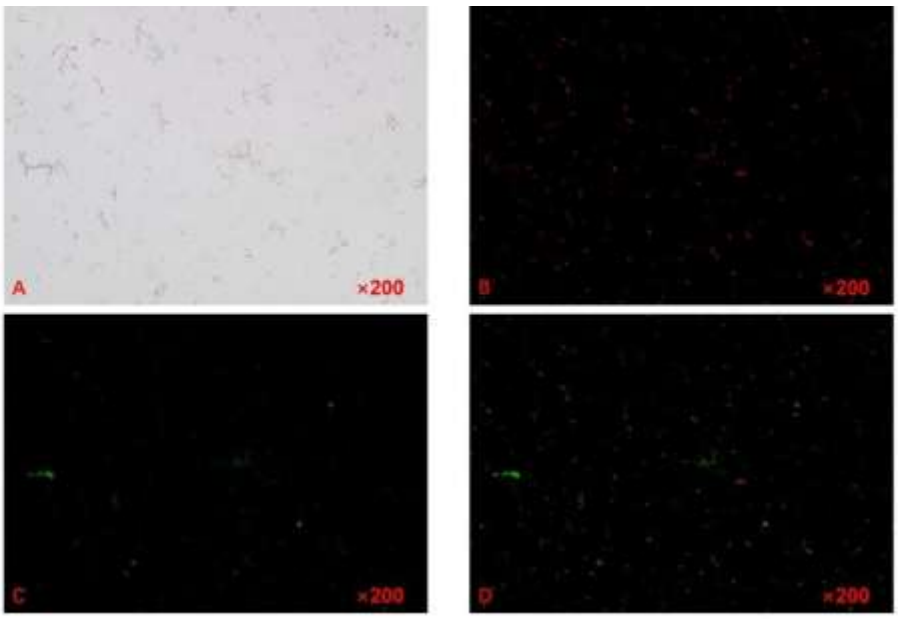

Figure 3.30 – Microscopic results of 36 h and 20-fold fixation of strain Hao 2022

As shown in Fig. 3.31, oil microscope observation showed a more concentrated field of view, with dense distribution of red fluorescence signal and green fluorescence signal, and obvious yellow overlapping area, indicating that there was a large degree of co-localization between bacterial surface polysaccharides and cell surface markers, which to a certain extent reflected the fact that bacteria wrapped themselves by EPS to form a protective matrix.

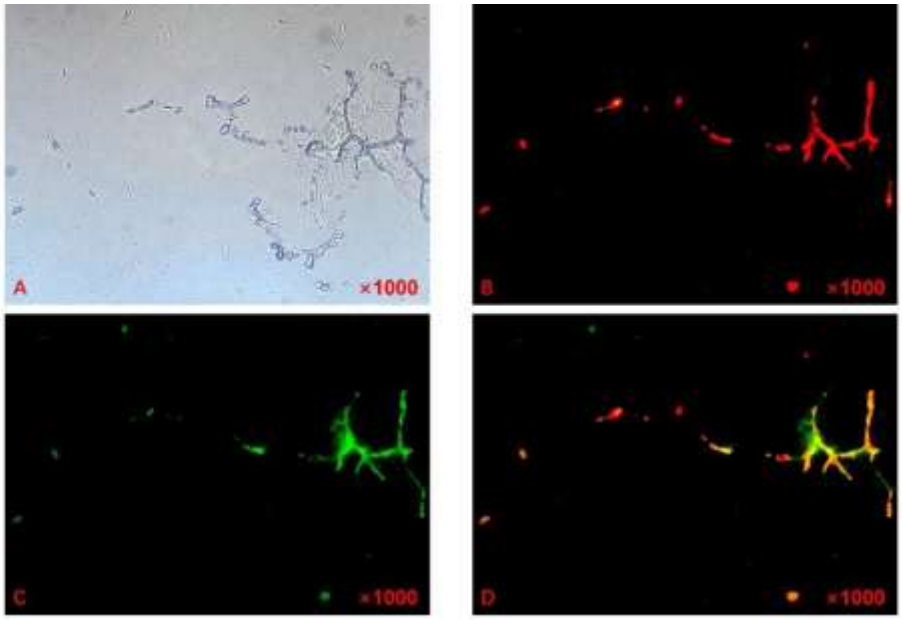

Figure 3.31 – Mirror results of 36 h and 100 times fixation of strain Hao 2022

As shown in Fig. 3.32, the red fluorescence signal was widely distributed, the green fluorescence signal was relatively dispersed and the double signals were weak, and the yellow overlapping area was not significant. It was possible that EPS might degrade because the bacterial sample was not fixed, the two-color dye was not completely penetrated, and the bacterial was in the decline phase.

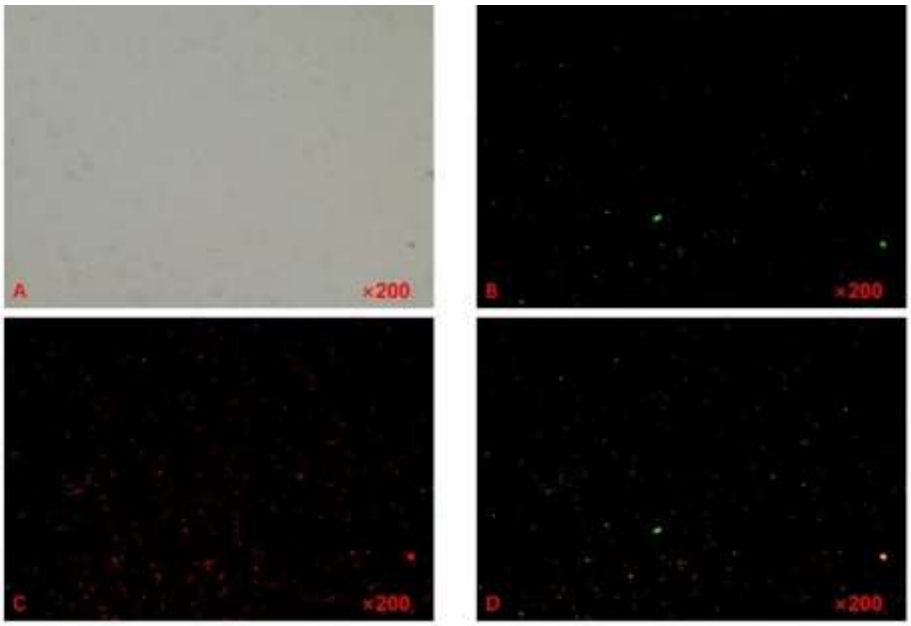

Figure 3.32 – Non-fixed 36h 20-fold microscopic result of strain Hao 2022

As shown in Fig. 3.33, the red-green fluorescence signal was distributed dispersedly and sparsely, and no yellow overlapping region was observed. The reasons might be that the bacterial sample was not fixed, the dye was not completely penetrated, and the bacterial cell was in the decline stage, cell lysis and EPS degradation.

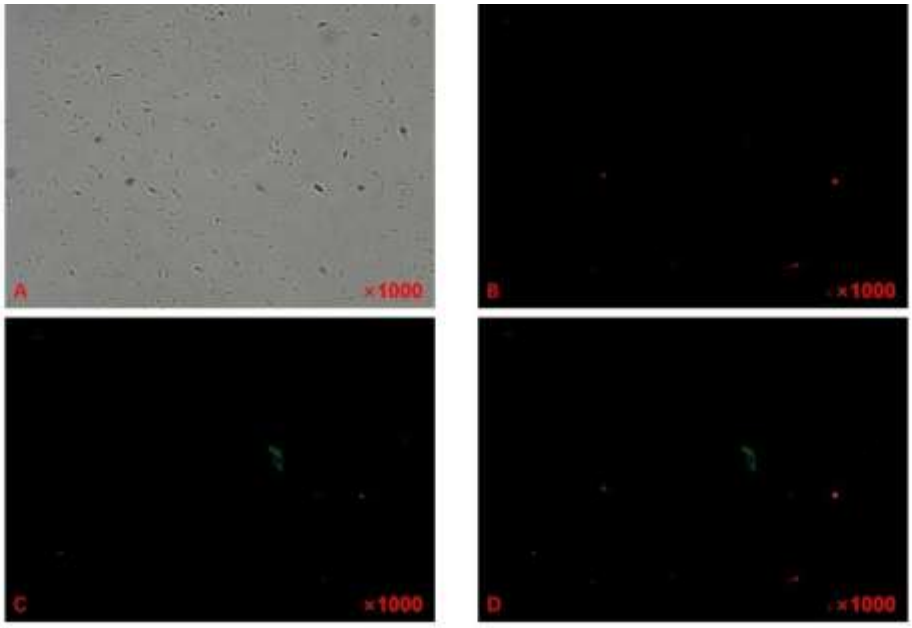

Figure 3.33 – Non-fixed 36h 100fold microscopic result of strain Hao 2022

3.5 Meta-*Bacillus halosaccharovorans* HAO 2023 observation

3.5.1 Observation on strain HAO 2023 4H

As shown in Fig. 3.34, the red fluorescence signals were scattered and plentiful, the green fluorescence signals were weak and few in number, and the yellow overlapping area was not significant, which might be due to the fact that the strain was in the delay period, with slow appreciation and small polysaccharide yield.

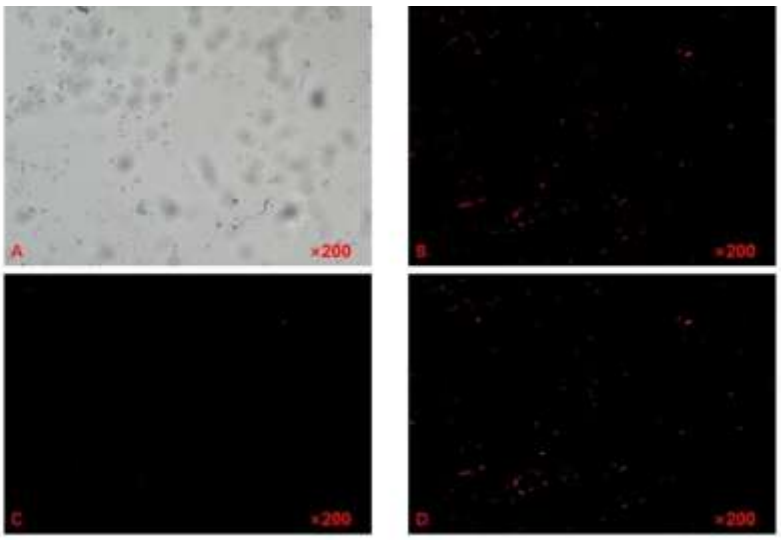

Figure 3.34 – Microscopic results of 4h 20-fold fixation of strain Hao 2023

As shown in Fig. 3.35, the red fluorescence signal and green fluorescence signal were distributed sporadically and the green signal was weak, indicating that the strain was in the delayed phase, with slow appreciation, small polysaccharide yield, and relatively obvious yellow overlapping area, indicating that there was a certain degree of co-localization between bacterial surface polysaccharides and cell surface markers.

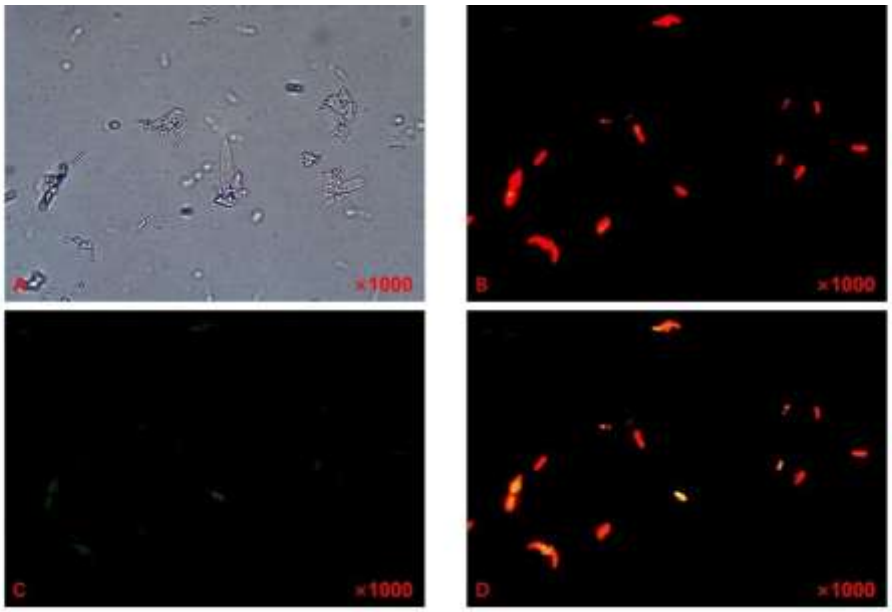

Figure 3.35 – Microscopic results of 4h 100-fold fixation of strain Hao 2023

As shown in Fig. 3.36, the red fluorescence signals were scattered and plentiful, the green fluorescence signals were few, the yellow overlapping area was not significant, the sample of strain was not fixed, and the living cells prevented dye penetration or the metabolic activities of the sample led to dye degradation.

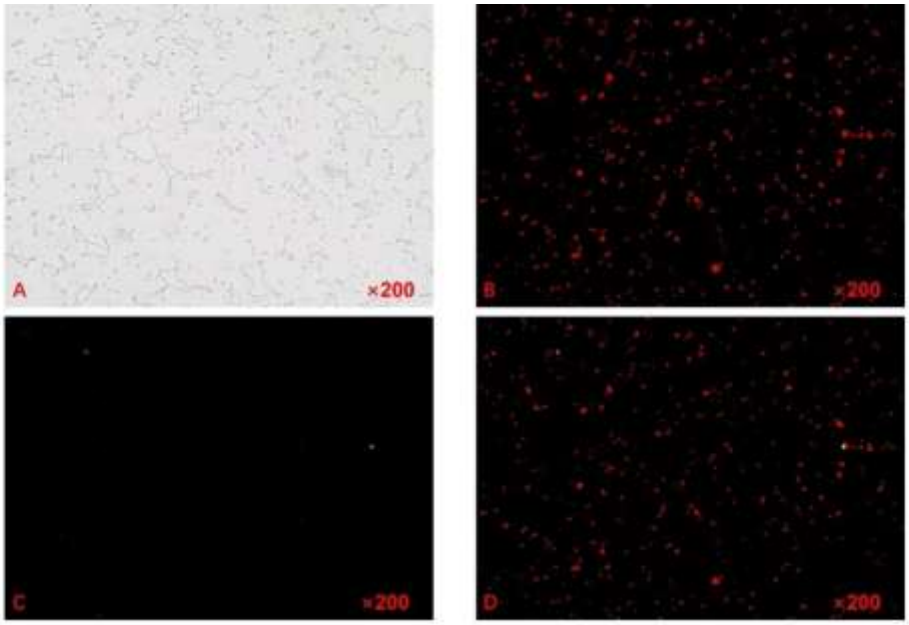

Figure 3.36 – Non-fixed 4h 20-fold microscopic result of strain Hao 2023

As shown in Fig. 3.37, the visual field of the oil microscope was relatively concentrated, the red fluorescence signal and green fluorescence signal were few and

scattered, the yellow overlapping area was not significant, the strain sample was not fixed, and the dye degradation was caused by living cells obstructing dye penetration or metabolic activity of the sample.

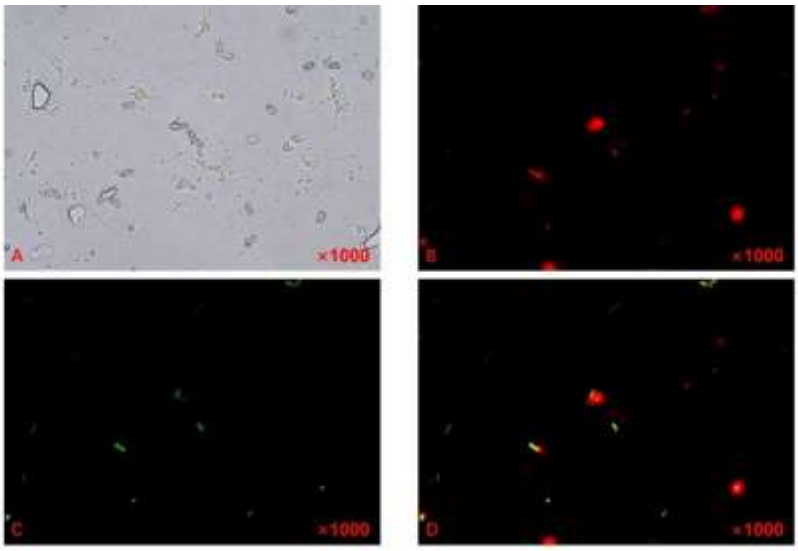

Fig. 3.37 – Non-fixed 4h 100-fold microscopic results of strain Hao 2023

3.5.2 Observation on strain HAO 2023 22H

As shown in Fig. 3.38, the red fluorescence signal was extremely rare, the green fluorescence signal was plentiful and dispersed, but the signal was weak, and the yellow overlapping area was not significant. It was possible that because the strain sample was in the delay period, the bacteria had not proliferated significantly, and some strains would secrete EPS in advance when adapting to the environment.

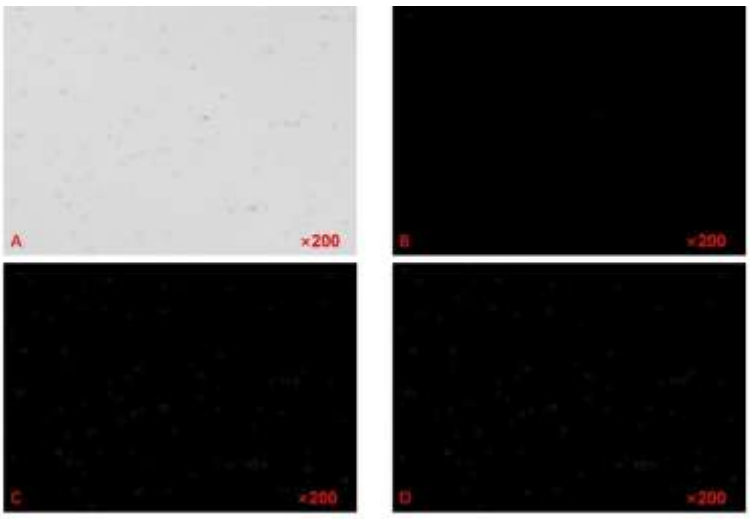

Fig. 3.38 – Twenty-fold microscopic results of 22h 20 fixation of strain Hao 2023

As shown in Fig. 3.39, the red and green fluorescence signals were not uniformly distributed, and the yellow overlapping area was relatively obvious, indicating that there was a certain degree of co-localization between bacterial surface polysaccharides and cell surface markers.

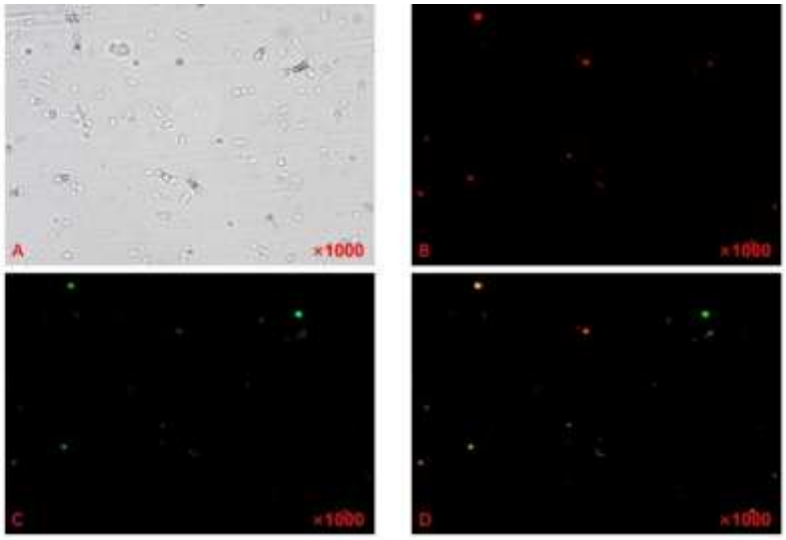

Fig. 3.39 – Results of 22h 100fold endoscopy of strain Hao 2023 fixation

As shown in Fig. 3.40, red and green fluorescence signals were few and distributed unevenly, and the yellow overlapping area was relatively obvious, indicating that there was a certain degree of co-localization between bacterial surface polysaccharides and cell surface markers, but the samples were not fixed, and living cells might lead to incomplete dye infiltration or dye metabolism.

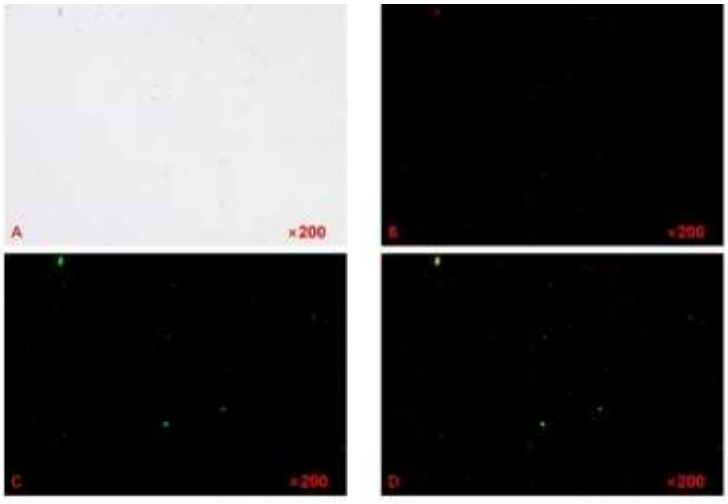

Fig. 3.40 – Non-fixed 22h 20fold microscopic results of strain Hao 2023

As shown in Fig. 3.41, the red-green fluorescence signals were few in number and dispersed, and the yellow overlapping area was not obvious. It was possible that the number of bacteria decreased and EPS gradually degraded due to the fact that the strain sample entered the decline phase, and microscope exposure or improper gain setting could not be ruled out.

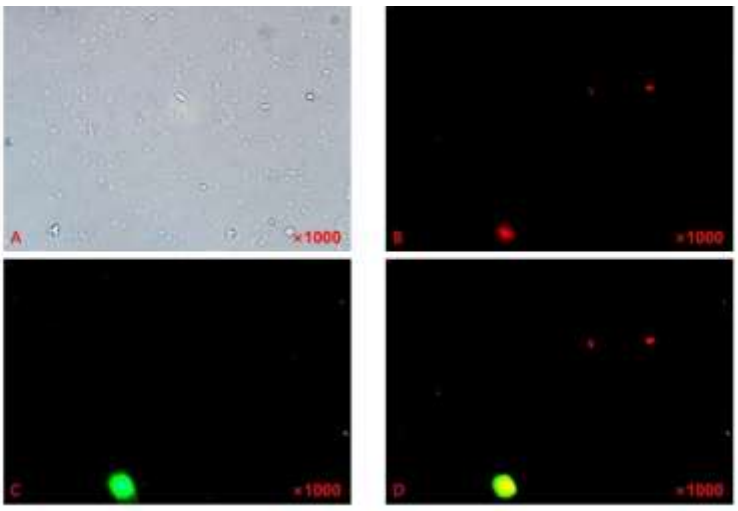

Fig. 3.41 – Non-fixed 22h 100fold microscopic result of strain Hao 2023

3.5.3 Observation on strain HAO 2023 36H

As shown in Fig. 3.42, the red-green fluorescence signals were extremely few and scattered, with weakened signals and indistinct yellow overlapping area. It was possible that the number of bacteria was decreased and EPS was gradually degraded due to the entering of the decline phase of strain samples, but microscope exposure or improper gain setting could not be ruled out.

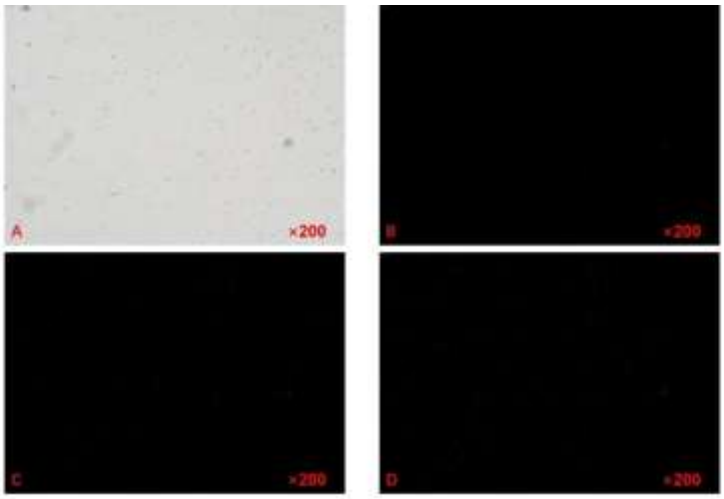

Fig. 3.42 – Twenty-fold microscopic results of 36 h fixation of strain Hao 2023

As shown in Fig. 3.43, the red-green fluorescence signals were few in number and dispersed, and the yellow overlapping area was not obvious. It was possible that the number of bacteria decreased and EPS was gradually degraded due to the fact that the strain sample entered the decline stage, and microscope exposure or improper gain setting could not be ruled out.

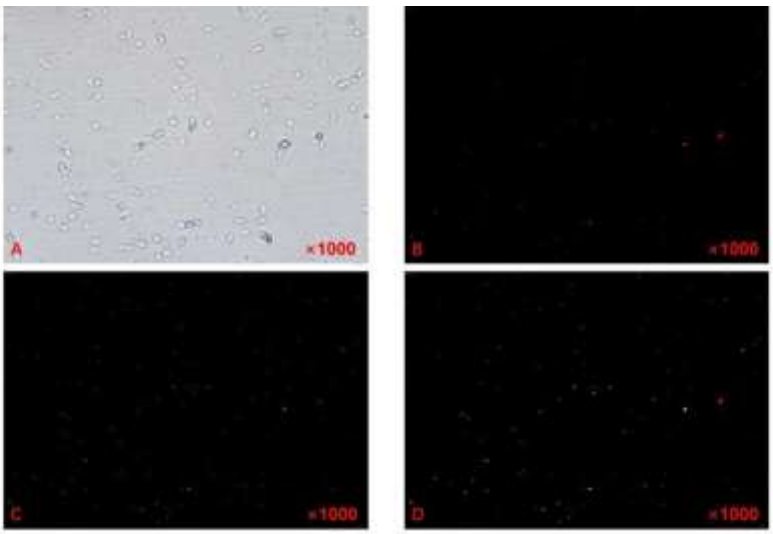

Fig. 3.43 – Mirror results of 36 h and 100 times fixation of strain Hao 2023

As shown in Fig. 3.44, the red-green fluorescence signals were few in number and dispersed, but the degree of coincidence was relatively high, and the yellow overlapping area was not significant. It was possible that the number of bacteria was decreased and EPS was gradually degraded when the strain sample entered the decline phase, and at the same time, the non-fixation of the sample affected the staining result.

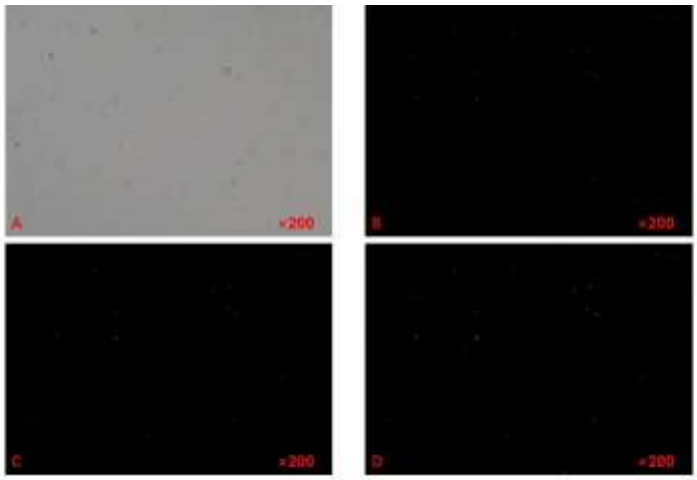

Fig. 3.44 – Twenty-fold microscopic results of non-fixed 36 h of strain Hao 2023

As shown in Fig. 3.45, the red-green fluorescence signals were few in number and dispersed, but the degree of coincidence was relatively high, and the yellow overlapping area was not significant. It was possible that the number of bacteria was decreased and EPS was gradually degraded when the strain sample entered the decline phase, and at the same time, the non-fixation of the sample affected the staining result.

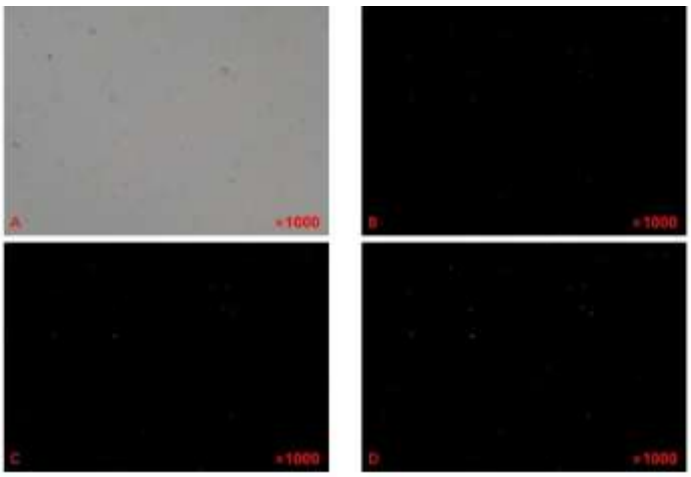

Fig. 3.45 – Non-fixed 36h 100-fold microscopic result of strain Hao 2023

3.6 *Staphylococcus pseudomonas* HAO 2024 OBSERVATION

3.6.1 Observation on strain HAO2024H

As shown in Fig. 3.46, the red fluorescence signals were distributed densely and in large numbers, while the green fluorescence signals were distributed dispersedly and in small numbers. The yellow overlapping area was not significant, which might be due to the fact that the strain was in the delay period and the yield of polysaccharides was small.

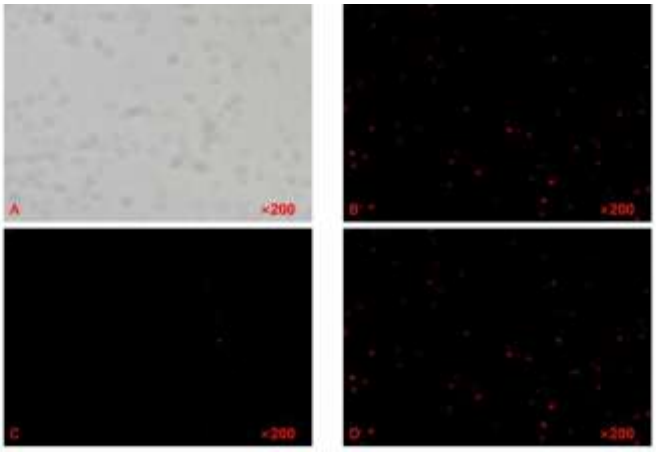

Fig. 3.46 – Results of 4h 20-fold endoscopy of strain Hao 2024 fixation

As shown in Fig. 3.47, the visual field of the oil microscope was relatively concentrated, with strong but scattered red fluorescence signal, few green fluorescence signals and insignificant yellow overlapping area. The reason might be that the strain was in the delay period and the yield of polysaccharide was small.

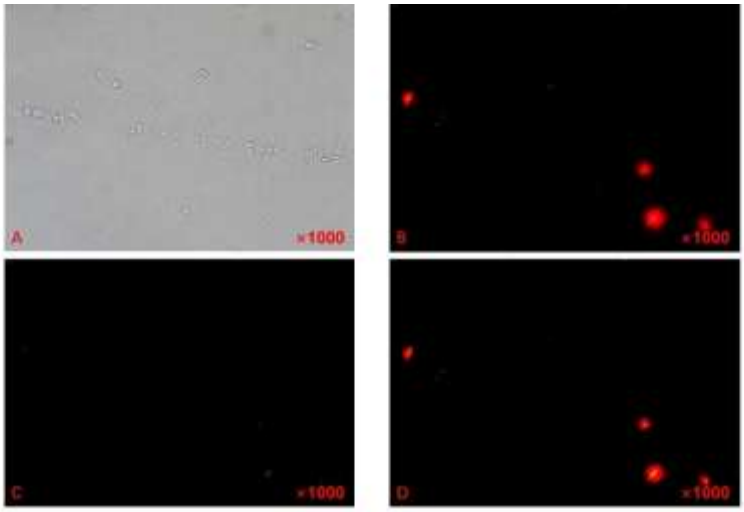

Fig. 3.47 – Results of 4h 100-fold endoscopy of strain Hao 2024 fixation

As shown in Fig. 3.48, the red fluorescence signal was dispersed, the number of green fluorescence signals was small, and the yellow overlapping area was not significant, which might be due to the fact that the strain was in the delay period, the yield of polysaccharide was small, and the sample was not fixed.

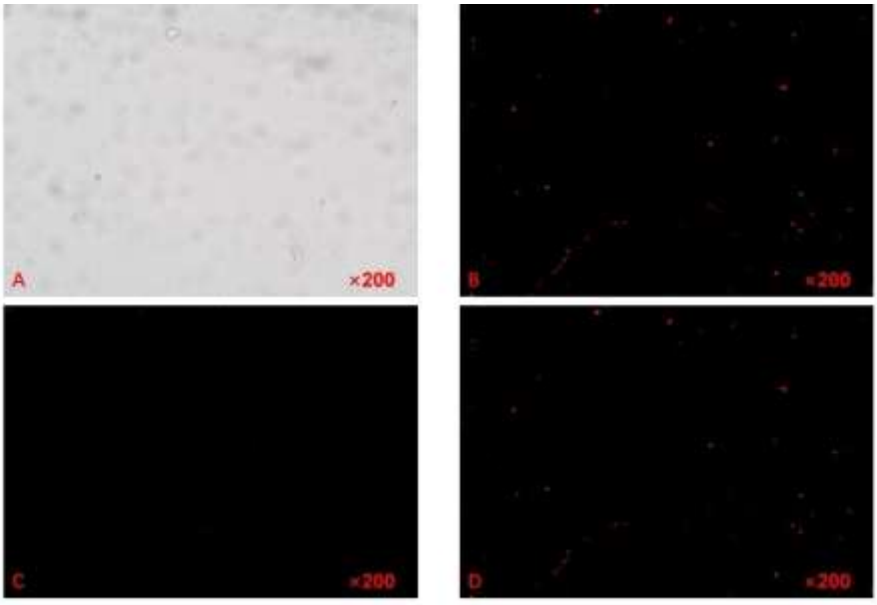

Fig. 3.48 – Non-fixed 4h 20-fold microscopic results of strain Hao 2024

As shown in Fig. 3.49, the field of view of the oil microscope was relatively concentrated, with weak red and green fluorescence signals, and insignificant yellow overlapping area. The reason might be that the strain was in the delay stage and the yield of polysaccharide was small.

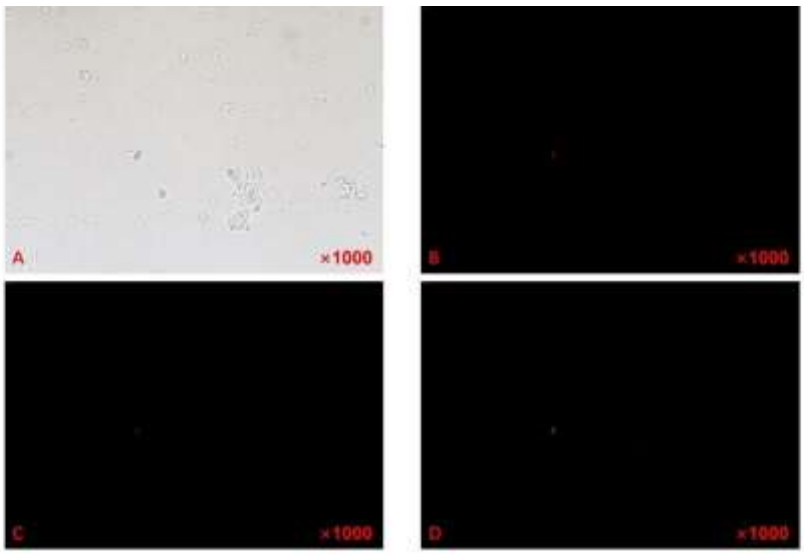

Fig. 3.49 – Non-fixed 4h 100-fold microscopic results of strain Hao 2024

3.6.2 Observation on strain HAO 2024 22H

As shown in Fig. 3.50, the red fluorescence signal was strong but dispersed, the number of green fluorescence signals was small, and the yellow overlapping area was not significant, which might be due to the fact that the strain was in a stable stage, the bacteria stopped proliferating but some strains were still actively metabolized, and the secretion of EPS was decreased.

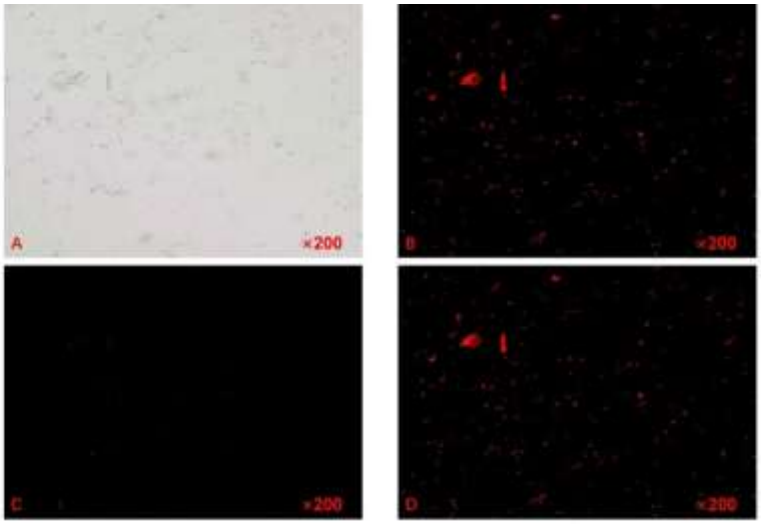

Fig. 3.50 – Results of 22h 20-fold endoscopy of strain Hao 2024 fixation

As shown in Fig. 3.51, the red-green fluorescence signals were strong but dispersed, and the yellow overlapping area was obvious, which might be due to the fact that the strain was in the stable stage, and the amount of EPS secreted by bacteria was small but highly concentrated on the surface of the bacteria, reflecting the state of bacteria -EPS interaction.

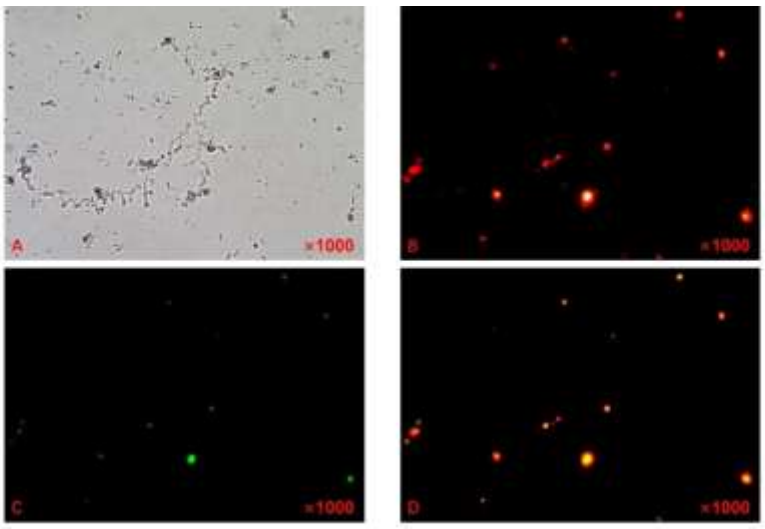

Fig. 3.51 – Results of 22h 100fold endoscopy of strain Hao 2024 fixation

As shown in Fig. 3.52, the red and green fluorescence signals were relatively scattered, with high degree of signal co-localization, and few yellow overlapping areas, which might be due to the imbalance of red and green signal strengths or the three-dimensional spatial dislocation caused by the living sample.

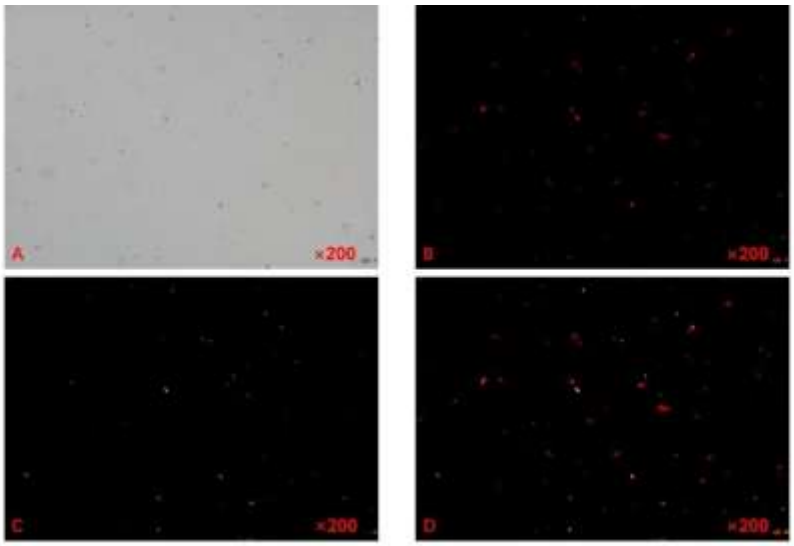

Fig. 3.52 – Results of 22h 20fold endoscopy of strain Hao 2024 without fixation

As shown in Fig. 3.53, the red-green fluorescence signal was strong but dispersed, with no yellow overlapping region. The reason might be that the strain was in the stable stage, and the secretion mode of bacterial EPS was changed. Bacteria released EPS directly to the surrounding environment rather than attaching to the cell surface, reflecting the state of bacterial -EPS interaction.

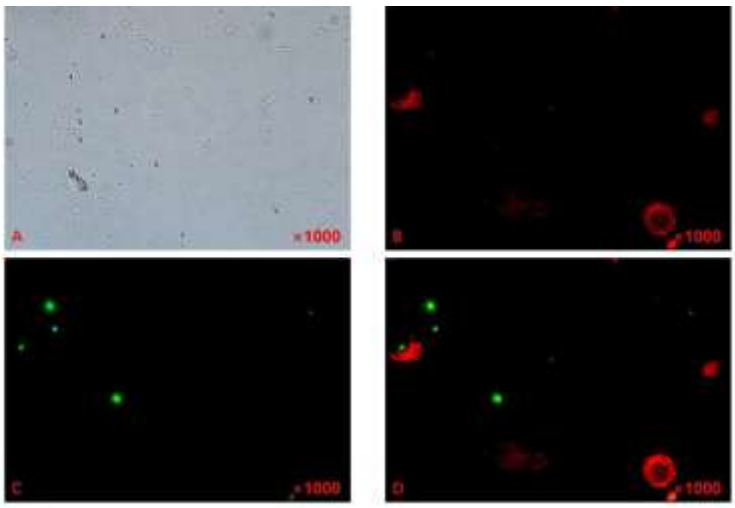

Fig. 3.53 – Non-fixed 22h 100fold microscopic results of strain Hao 2024

3.6.3 Observation onstrain HAO 2024 36H

As shown in Fig. 3.54, the red-green fluorescence signals were few in number and dispersed, with weakened signals and indistinct yellow overlapping area. It was possible that the number of bacteria was decreased and EPS was gradually degraded due to the entering of the decline stage of strain samples, but microscope exposure or improper gain setting could not be ruled out.

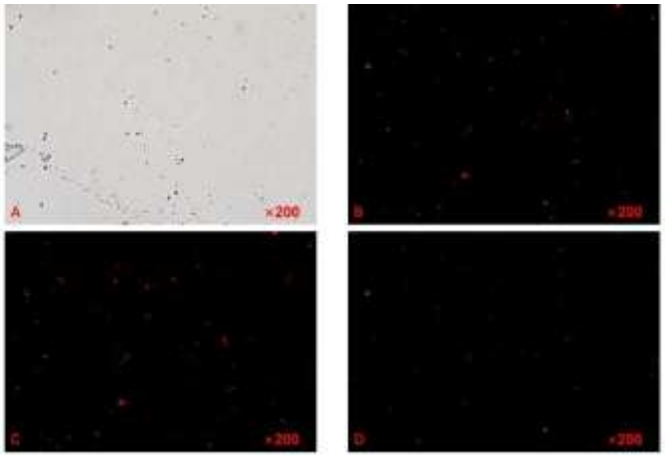

Fig. 3.54 – Results of 36h 20-fold endoscopy of strain Hao 2024 fixation

As shown in Fig. 3.55, the red and green fluorescence signals were strong but dispersed, with no yellow overlapping area. The reason might be that the strain was in the decline and fall stage, the secretion of bacterial EPS was decreased, and the oil microscopic field of view was narrow and distributed unevenly.

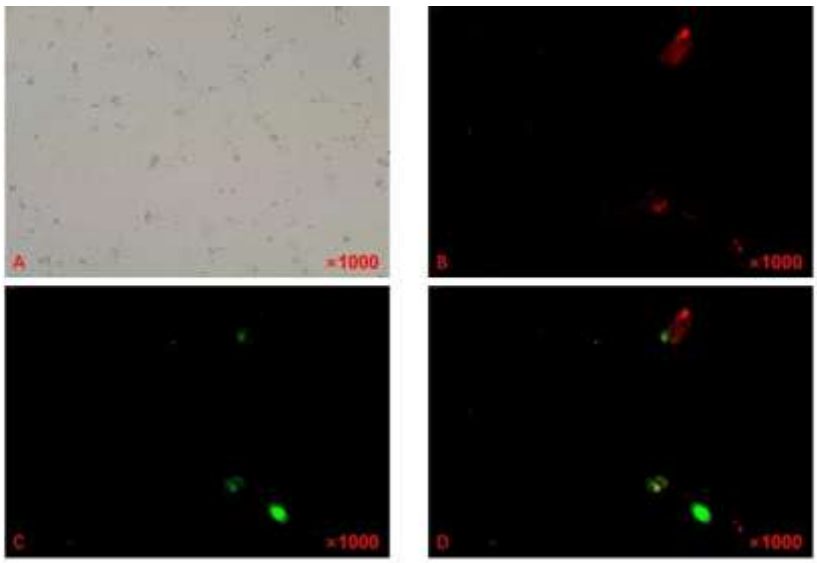

Fig. 3.55 – Results of 36h 100-fold endoscopy of strain Hao 2024 fixation

As shown in Fig. 3.56, the red-green fluorescence signals were less in number and dispersed, with low coincidence degree, and the yellow overlapping area was not significant. It was possible that the number of bacteria was decreased and EPS was gradually degraded when the strain sample entered the decline phase, and meanwhile, the non-fixation of the sample affected the staining result.

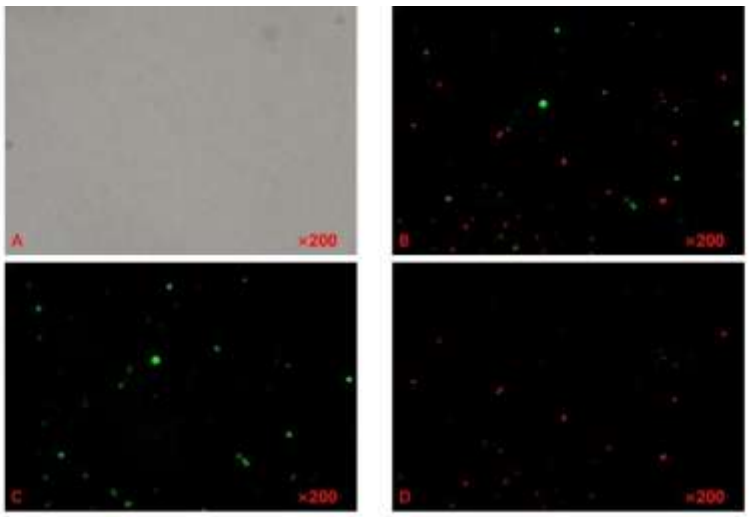

Fig. 3.56 – Non-fixed 36h 20-fold microscopic result of strain Hao 2024

As shown in Fig. 3.57, oil microscope observation showed a higher resolution. The red and green fluorescence signals were relatively strong but dispersed, with a very low degree of coincidence, and no yellow overlapping area was observed. It was possible that the number of bacteria was decreased and EPS was gradually degraded when the strain sample entered the decline stage, while the sample was not fixed, which affected the staining effect.

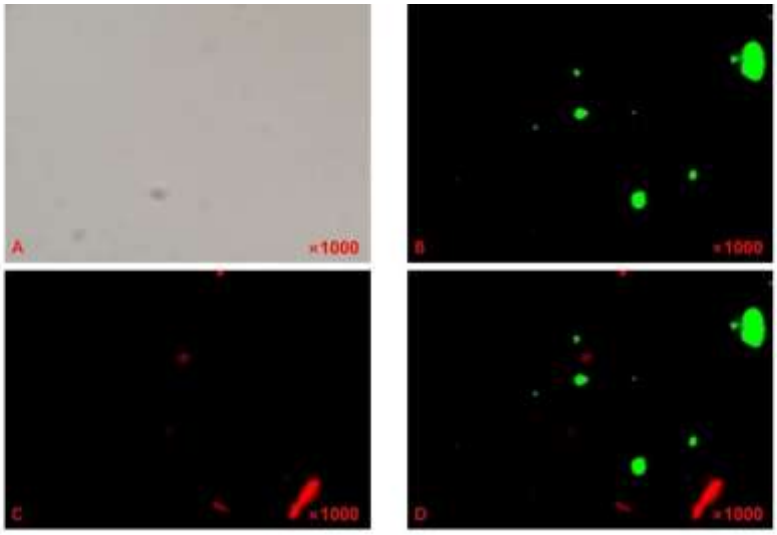

Fig. 3.57 – Non-fixed 36h 100fold microscopic results of strain Hao 2024

3.7 Microscopic observation and analysis

The images in this chapter contain transmission electron microscope images of three time periods from a sample of exopolysaccharides from marine bacterium Hao 2018. The polymer of a. pseudoalternans Hao 2018 use macromolecular chains as a basi and branch derivatization as a connection mode, and different polymers are connected with each other to form a network arrangement, wherein that contact mode of sugar molecular units is not single, so that a plurality of branch with different shapes are derived, the size range is floating within 20 to 110 nm, and the chemical structure of an extracellular polysaccharide macromolecule is highly branched[8].

3.7.1 Observation of strain HAO 2018 4H

As shown in Figs. 3.58 and 3.59, two main cell morphologies could be seen: the rod-shaped cells were elliptical-cylindrical, with a long size, and some had obvious

medial axis structure; Spherical or subglobose cells were small in size, neatly contoured, and showed clear differences in central density, suspicious for inclusions or nuclear regions; The scale in the figure shows 1 μm, and the length of rod-shaped bacteria can be estimated to be about 2–4 m, and the diameter of spherical bacteria is about 0.8-1.5 μm ;; Most cells showed uniform electron density, and some cells showed high density or bright spots in the central region, which might be formed by DNA aggregation or inclusions. The overall image showed that most of the cells had clear outlines, and the cell wall boundaries were continuous, without significant damage or outflow of contents. Very few cell boundaries are slightly blurred but do not constitute significant evidence of cell lysis; There were no significant signs of cytoplasmic leakage or rupture, indicating that the cell walls remained generally intact after 4 hours of culture, indicating a mild environment and a stable bacterial state. In both images, slight contraction or dark line-like structure was observed in the middle part of individual rod-shaped bacteria, which was suspected to be undergoing cell division. There were no typical fissures or "septal structures", and it was speculated that most cells had not yet or just begun to divide; Paired arrangement or obvious cleavage furrows were not observed in spherical cells, which might be in quiescence or early growth phase.

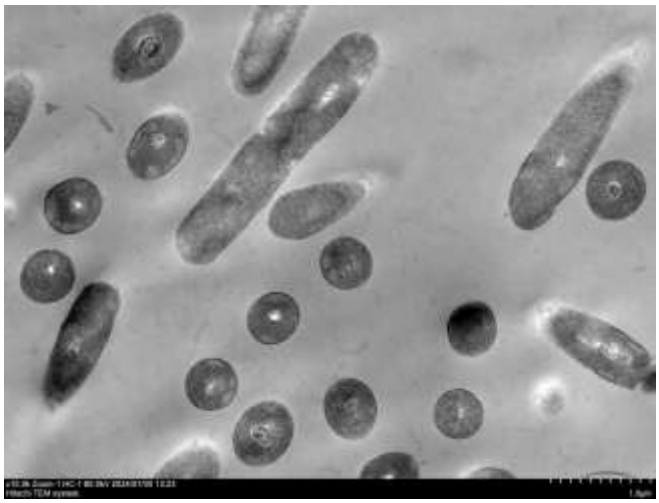

Fig. 3.58 – Image of strain Hao 2018 4h

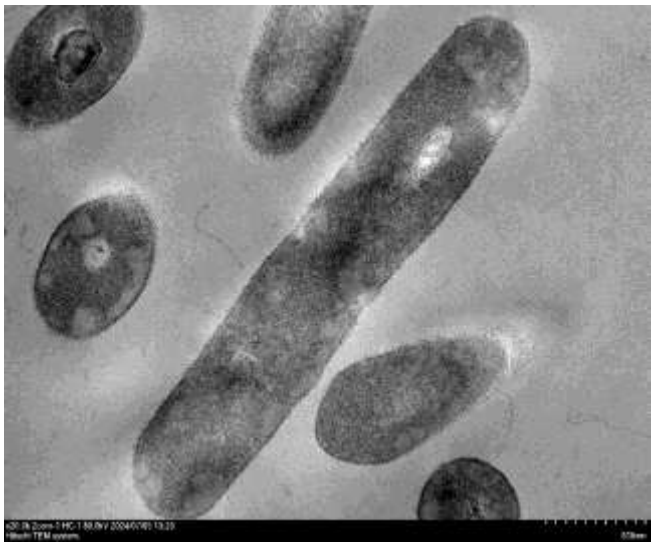

Fig. 3.59 – Image of strain Hao 2018 4h

3.6.2 Observation of strain HAO 2018 22H

As shown in Figs. 3.60 and 3.61, most of the cells had clear outlines and high electron density at the boundary, indicating that the cell wall structure was intact, and no obvious rupture or cytoplasmic leakage was observed, indicating that the cells were in a relatively healthy physiological state. Some cells had slightly vague edges or slight structural deformation, which might be related to mitotic activities or stress response. Some cells exhibited typical mitotic characteristics, such as constrictions in the center, pale fissures, or "bicellular" structures, suggesting an active binary fission process. Most of the cells were still in a non-dividing state, indicating that the bacterial population division was asynchronous and in different cell cycle stages. A large number of filamentous structures, possibly flagella, fimbriae or extracellular DNA fragments, could be seen around the cells, suggesting that the strain had potential locomotor ability or population behavior (such as biofilm formation). High electron density particles were observed in some cells, which might be storage particles or inclusion bodies, reflecting their metabolic activities.

Fig. 3.60 – Image of strain Hao 2018 22h

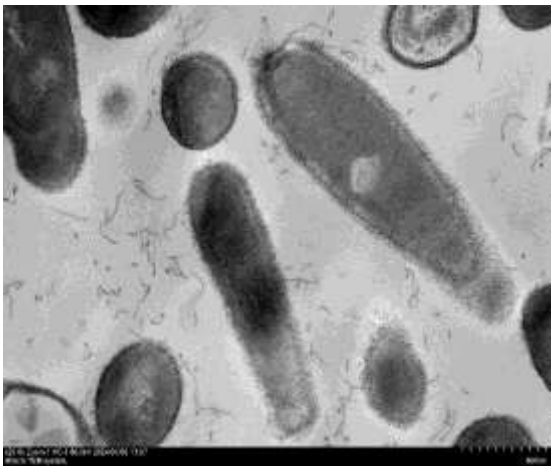

Fig. 3.61 – Image of strain Hao 2018 22h

3.6.3 Observation of strain HAO 2018 FOR 36 H

As shown in Figs. 3.62 and 3.63, most of the cells had clear and complete double-layer structure boundaries, showing that the cell wall structure was intact, and no obvious cleavage, damage or collapse was observed. The outline of a few cells was slightly vague, and it was speculated that they might be in a state of cytoplasmic contraction or early decline. In addition, some cells show the characteristics of dense edges and sparse center, which may be the thick-walled structure or in the early stage of endospore formation. The typical binary fission metaphase structure, such as obvious constrictions or the formation of dividing septa, was not observed. Although some cells were large in size and elongated in morphology, which might be the pre-state of cell division, no large number of cells were in the division stage at the same time on the whole, indicating that the flora as a whole was in a stable growth period or

had entered the growth slowdown stage at the current time point (36h). The morphology of strain Hao 2018 was stable after 36-h culture, mainly in the form of short rods, and the cell wall structure was generally intact. No large number of synchronous divisions were observed, suggesting that this time point might be in a stage of metabolic balance or transition to a recession. Some cells with special structures deserve further study and may involve sporulation or heterogeneous cell populations.

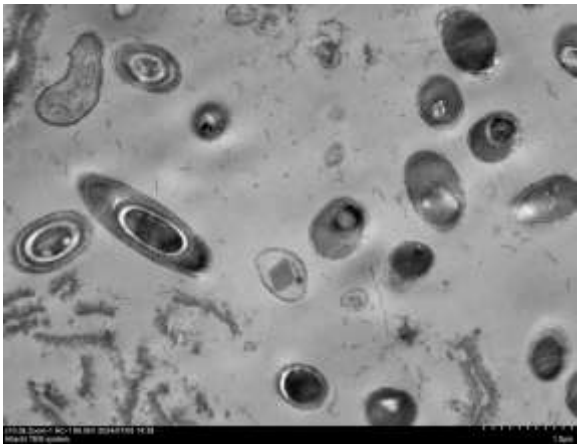

Fig. 3.62 – Image of strain Hao 2018 36h

Fig. 3.63 – Image of strain Hao 2018 36h

Conclusions to chapter 3

Polysaccharides and their complexes are one of the abundant natural macromolecular substances from higher plants, animal cell membranes and microbial cell walls. They are closely related to human life and play a vital role in maintaining life activities. protein, nucleic acid and lipid constitute the most basic four kinds of

living substances.[14]. In this chapter, the interaction of bacteria and extracellular polysaccharide (EPS) in fixed and non-fixed living samples was systematically studied by laser confocal microscopy, with emphasis on the strength of red and green fluorescence signals, the causes of non-overlapping phenomenon and its biological significance. Studies have found that bacteria at specific growth stages or environmental conditions may tend to secrete free EPS rather than attaching it to the cell surface, resulting in the absence of co-localization signals. This phenomenon is closely related to the physiological state of bacteria (such as preferential proliferation in logarithmic phase) and environmental stress (such as high salt and shearing force). For technical optimization, false-negative results due to staining efficiency, optical errors, or channel crosstalk were excluded through dye screening, three-dimensional imaging, and spectral calibration.

Biologically speaking, the secretion strategy of bacterial free-form EPS may have important ecological adaptive value. This secretion pattern could not only form an extracellular matrix conducive to nutrition capture, but also avoid cell activity limitation caused by excessive encapsulation of EPS. In the marine environment, free EPS may enhance the environmental adaptability of bacteria by chelating metal ions and regulating local osmotic pressure. However, the molecular mechanism of dynamic regulation of EPS secretion is still not fully understood, especially how the environmental signals are converted into regulatory instructions for the synthesis and secretion of EPS needs further investigation.

With the passage of culture time, bacterial morphology, structural integrity and population state changed significantly. The bacteria cultured for 4 h mainly showed rod-shaped and spherical forms. The rod-shaped cells were regular, with smooth surface and uniform cytoplasm. The overall structure was healthy and stable. Most cell walls were clear and complete in outline, and a small number of cells might be entering a division state, showing a slight bright band in the middle of some cells, which was an early manifestation of cell constriction, indicating that the bacteria were in an early logarithmic phase. By 22 hours, the bacterial morphology was mainly elliptical to rod-shaped, which was more densely arranged. More cells showed typical division

characteristics, and the cell wall was in good integrity. No structural damage or membrane rupture was observed, and the overall state was active. At this stage, the flora was in an active mitotic stage, and visible in the image were some cells with obvious central constriction or cleavage, and the metabolic activity of the cell population was high. In the 36-hour sample, the bacteria were still mainly in the form of short rods, but some cells showed vague outlines or slightly deformed edges, suggesting that some cells began to enter the quiescent phase or the aging process. Although most cells still maintained intact cell wall structures, the number of splinter cell was significantly reduced as compared with that in the early stage, suggesting that the growth rate of the flora was decreased. In addition, dark accumulation regions appeared in some cells, which might be the manifestations of energy storage particles or cytoplasmic concentration, and cell metabolism entered a slowing stage.

From the observation of extracellular polysaccharide, no obvious extracellular polysaccharide structure was observed in the 4-hour sample, and the surrounding cells were relatively clean, indicating that the bacteria had not secreted a large amount of extracellular matrix. By 22 hours, fuzzy edges or coating layers appeared around some cells, and filamentous or gel-like structures appeared in the background, indicating that extracellular polysaccharide began to be secreted, which might be related to the early formation of biofilm or regulation of population behavior. By 36 hours, the accumulation of extracellular polysaccharide was more significant. Some cells were surrounded by dense extracellular substances, and more secretion deposits could be seen in the background, indicating that bacteria might enhance their stability, resist environmental stress or support the maturation and formation of biofilm by synthesizing extracellular polysaccharides at this stage. In summary, the secretion of exopolysaccharides gradually increased with the passage of time, which was consistent with the process of bacterial population from rapid growth phase to stable phase.

CONCLUSIONS

The structural characteristics of exopolysaccharides of four marine bacteria were studied, and the results showed that the strains Hao 2018, Hao 2022, Hao 2023 and Hao 2024 had both similarities and differences. First, the growth kinetics of four marine bacteria were studied. After continuously measuring OD600 of four marine bacteria within 36h, the growth curves of four marine bacteria were drawn, and the results showed that the physiological characteristics of four marine bacteria were similar under the culture condition of 25℃, and strain Hao 2018 and strain Hao 2024 had similar growth cycles. Secondly, the exopolysaccharide production of the two marine bacteria was measured by the phenol-sulfuric acid method, and the results showed that the exopolysaccharide production of the four marine bacteria in their stable stage was different, with the interval of about 0.18 g/L to 0.4 g/L. Finally, systematic observation of extracellular polysaccharide (EPS) under laser scanning confocal microscope and transmission electron microscope revealed that EPS exhibited significant spatial heterogeneity in terms of distribution characteristics, mainly accumulating around bacterial cells and in the intercellular space of colonies, forming fibrous network or granular aggregation structures with biological significance. Especially, in the biofilm system, EPS exhibited a complex three-dimensional configuration, and there were significant differences in the density and chemical composition of each region. High-resolution co-localization analysis revealed the dynamic interaction between bacteria and EPS, including surface binding, polar secretion and other characteristic phenomena, and this interaction showed a significant time dependence, which was gradually enhanced with the prolongation of culture time. Microbial polysaccharide is a new product of microbial fermentation industry. It is more widely used than animal polysaccharide and plant polysaccharide. Besides, its production is less affected by factors such as geographical environment, climate, natural disasters and so on. The production cycle is short. The yield and quality are very stable. The cost-performance ratio is high. Its various performance is not only excellent but also has special functions that other polysaccharides do not have. With the continuous improvement of

production technology, microbial polysaccharides in the industrial application will continue to broaden the scope of[9]. In summary, the results of this study are of great significance for further understanding of these marine bacteria exopolysaccharides and provide a theoretical basis for the selection of fermentation production methods of exopolysaccharides

In this study, four representative bacteria were selected as the research object, aiming to determine the growth curve of their extracellular polysaccharide synthesis process and dynamically grasp the relationship between bacterial growth and extracellular polysaccharide synthesis. At the same time, the cellular characteristics of exopolysaccharides were analyzed at the micro level by laser scanning confocal microscope and transmission electron microscope technology, which provided a theoretical basis for revealing the synthetic mechanism of exopolysaccharides and optimizing the production process. However, there are still some limitations in this study, which need to be further improved. Specifically as follows:

First, the sample size in this study was small, and only four marine bacteria were selected for study, which could not represent the structural characteristics of the entire marine bacterial community. On this basis, in the future research, the number of samples can be increased to conduct a more comprehensive and in-depth study on marine bacteria of different types and different environments, so as to sum up the common characteristics of marine bacteria and guide production practice.

Secondly, traditional methods such as staining observation, growth curve drawing and AFM research at the cell level are adopted in this study, which have certain limitations on some minor details and the fine connection between bacteria and other organelles. Therefore, in the future research, modern technologies and methods such as high-resolution microscopy and single-cell sequencing technology can be combined to more comprehensively and accurately study other structural characteristics of marine bacteria.

Thirdly, the future research is expected to reveal the spatio-temporal dynamics of bacterial -EPS interaction by further combining microfluidic technology with in vivo dynamic imaging. The molecular regulatory network behind the non-overlapping

signals was analyzed by multi-group consortium (such as the combination of transcriptome and fluorescence microscopy). The structure of the bacteria -EPS interface was characterized at the nano-scale by ultra-high resolution microscopy (such as STORM). In addition, the ecological function of free EPS (such as carbon cycle contribution) and its role in the early stage of biofilm formation deserve to be further explored[12]This study has provided a new perspective for understanding microbial-environmental interactions and the subsequent work can be extended to verification and application in complex natural systems such as marine microbial communities.

REFERENCES

1. Elena López, Israel Ramos, Ma Angeles Sanromán.Extracellular polysaccharides production by Arthrobacter viscosus. [J]. Journal of Food Engineering ,2003,60: 463-467.
2. Li Jiang, Chen Kaoshan, Hao Linhua, et al. Research progress of bacterial exopolysaccharides. Marine Science, 2006, 30(4): 74-77.
3. Chen Jingxiang, Sun Fengjun, Liu Songqing, Xia Peiyuan. Methodological research on observation of bacterial biofilm formation by laser scanning confocal microscope [J]. Modern Biomedical Progress, 2007,(05):653-655.
4. Hang Thi Nguyen,Lisa A.O'Donovan,Henrietta Venter, et al. Comparison of Two Transmission Electron Microscopy Methods to Visualize Drug-Induced Alterations of Gram-Negative Bacterial Morphology [J]. Antibiotics-Basel, 2021,10(3): 307-307.
5. Kirkelund S H ,B P R ,J A J H , et al.Evolution of species interactions in a biofilm community.[J]. Nature, 2007,445(7127): 533-6.
6. GE Jianping. Comparison of exopolysaccharide production by Actinomyces viscosus in biofilm and plankton [D]. Sichuan: Sichuan University, 2004.
7. Yin D , Zhong Y ,Hu J .Microbial polysaccharides biosynthesis and their regulatory strategies. [J]. International journal of biological macromolecules, 2025, 143013.
8. Liu Wenlin. Advanced Structure Analysis of Extracellular Polysaccharides from *Pseudoalteromonas agarivers* HAO 2018: Construction of Polysaccharides Metabolic Pathway and Mining and Analysis of Related Genes [D]. Qilu University of Technology, 2021.
9. Guo Min, Zhang Baoshan, Jin Xiaohui. Research progress of polysaccharide production by microbial fermentation [J]. Acta Microbiology, 2008, 35 (7): 1084-1090.
10. Li SW. Screening of extracellular polysaccharide-producing Kefir lactic acid bacteria and effects of yeast and acetic acid bacteria on their growth and metabolism [D]. Inner Mongolia Agricultural University, 2024. DOI: 10.27229/D.

CN KI. GN MNU.2024.001195.

11. Zhang Xiaofei. Screening of marine polysaccharide-producing bacteria and study on polysaccharide fermentation [D]. Shandong University of Light Industry, 2012.
12. LIU Yan-feng, ZHOU Jia-hao, YAN Xin-yu, et al. Research progress on action mechanism of extracellular polymeric substances (EPS) stabilizing soil aggregates and organic carbon [J/OL]. Zhejiang Agricultural Journal, 1-18 [2025-05-12]. http://kns.cnki.net/kcms/detail/33.1151.s.20250328.1128.002.html.
13. Xie Mingyong, Nie Shaoping. Research progress on structure and function of natural active polysaccharides [J]. China Journal of Food Science, 2010,10 (02): 1-11. DOI: 10.16429/J.1009-7848.2010.02.035.
14. Lowe B J , Marth D J .A GENETIC APPROACH TO MAMMALIAN GLYCAN FUNCTION[J].Annual Review of Biochemistry,2003,72(1):643-691.
15. A K K .The human gastric colonizer Helicobacter pylori: a challenge for host-parasite glycobiology.[J].Glycobiology,2000,10(8):761-71.
16. Liu Caie, Shi Wenhui, Feng Changchun, et al. Research on the key technology and quality evaluation method of whole plant corn silage [J]. Modern Livestock Technology, 2025, (05): 64-66. DOI: 10.19369/J. CN KI.2095-9737.2025.05.019.
17. Song Yan, Yao Kaiyue, Xu Jing, et al. Effects of extracellular polysaccharides of Sphingomonas on oleic acid-induced glucolipid metabolic disorders in IR-HepG2 cells [J/OL]. Acta Microbiologica Sinica, 1-21 [2025-05-24]. https://doi.org/10.13343/j.cnki.wsxb.20240813.
18. Liang SX, Zhang Chen, Li BQ, et al. The negative regulatory effect of ScvL on the biofilm formation of vibrio parahaemolyticus [J/OL]. Journal of Aquatic Biology, 1-9 [2025-05-24]. http://kns.cnki.net/kCMS/detail/42.1230.q.20250520.0956.002.html.
19. Yu Qunfang, Zhang He, Qi Yanxiang, et al. Whole genome sequencing and comparative genomics analysis of XcmL5, a pathogen of mango bacterial black spot [J/OL]. Molecular Plant Breeding, 1-23 [2025-05-24]. http://kns.cnki.net/kcms/detail/46.1068.s.20250520.1105.002.html.
20. Li Shuangxiong, Yao Tuo, Chai Jiali, et al. effect of that addition of compound

microbial inoculum on the physicochemical property of degraded alpine meadow soil [J/OL]. grassland and turfgrass, 1-13 [2025-05-24]. http://kns. cnki. net/kcms/detail/62.1156. S. 20250519. 1357. 002. html.

21. Wu Yating, Liu Yu, Meilin. Effects of Pediococcus lactis S1 on the antioxidant activity of myofibrillar protein [J/OL]. Journal of Anhui Agricultural University, 1-9 [2025-05-24]. https://doi.org/10.13610/j.cnki.1672-352x.20250519.020.
22. CHEN Xianrui, Wu Yanling, LIN Jiasheng, et al. Research progress on pathogenesis and control technology of citrus yellow dragon disease [J/OL]. Guangxi Science, 1-12 [2025-05-24]. HTTPS://DOI.org/10.13656/J.CN KI.GXKX.20250523.001.
23. Zhang Li, Cui Yaoming, Wang Qiumei, et al. Study on the effect of probiotics on promoting the proliferation and differentiation of intestinal epithelial cells [J/OL]. Feed Research, 1-13 [2025-05-24]. http://kns.cnki.net/kcms/detail/11.2114.s.20250514.1528.002.html.
24. Chen Genwang, Liu Lei, Huang Jiaming, et al. In vitro inhibitory effect of extracts of plantain on biofilm formation of Staphylococcus aureus [J]. Jilin Medical Science, 2025, 46(05):1025-1028.
25. LI Shu-ya, WU Yi-qing, Zhang Liping, et al. Screening of Co-cultured Lactic Acid Bacteria from a Metabolic Perspective and Study on Its Mechanism [J/OL]. Food and Fermentation Industry, 1-14 [2025-05-24]. HTTPS://DOI.org/10.13995/J. CN Ki.11-1802/TS.042363.
26. Li Zhongyang, Ma Shifeng, Geng Shixia, et al. Research progress on preparation technology of bioactive peptides and their application in aquatic feed [J]. Feed Industry, 2025, 46 (09): 132-141. DOI: 10.13302/J. CN KI. FI.2025.09.020.
27. GONG Xi, Zhao Yuxi, Tong Man, et al. Effects of chemical oxidation of different forms of Fe(Ⅱ) on the biological reduction of nitrate [J/OL]. Environmental Science and Technology, 1-11 [2025-05-24]. http://kns.cnki.net/kcms/detail/42.1245.x.20250509.1305.002.html.
28. Zhao Yujie, Johnny, Pan Xuewei, et al. Molecular mechanisms of CpxA/R two-component system participating in the regulation of physiological

characteristics of Serratia marcescens [J/OL]. Journal of Applied and Environmental Biology, 1-18 [2025-05-24]. https://doi.org/10.19675/j.cnki.1006-687x.2024.11045.

29. LIU Bo-lang, ZHANG Yi-tian, XIAO Pan, et al. Analysis of probiotic characteristics of four strains of Lactobacillus coil isolated from Huaixiang chicken [J/OL]. Feed research, 1-23 [2025-05-24]. http://kns.cnki.net/kcms/detail/11.2114.s.20250502.1840.002.html.
30. LU Han-chi, Wen Hao, Yu Yang, et al. Research progress on biological function and application of metaplasia [J]. Journal of Food Safety and Quality Testing, 2025, 16 (09): 1-11. DOI: 10.19812/J. CN KI. JFS Q11-5956/TS.2025011601.
31. Xu Jingyi, Fu Zhihong, Yi ZQ, et al. Mechanism and application of microbial-mediated remediation of heavy metal-organic composite pollution in water [J]. Journal of Nanchang University (Science Edition), 2025, 49 (02): 222-232. DOI: 10.13764/j. CN Ki. NCDL.2025.02.011.
32. GUO Ke-yu, Zhang Kai, YANG Liu, et al. Study on Growth-promoting Characteristics and Fermentation Optimization of Cotton under Saline-alkali Stress by Xanthomonas campestris L6 [J]. Northwest China Agricultural Journal, 2025,34(04):639-652.
33. Sun Ying, Wu Yiu Zhou, Wang Rui Rui, et al. Research progress on potential mechanisms and applications of non-antibacterial anti-infection therapy [J/OL]. chinese journal of nosocomiology, 2025, (11): 1735-1742 [2025-05-24]. http://kns.cn ki.net/kcms/detail/11.3436.r.20250423.1437.046.html.
34. Zhao Cheng, Huang Baijun, Zhang Xuan, et al. Microbial flocculant production and gene prediction of synthetic pathway by Paenibacillus polymyxa GA1 using oil-tea cake as a substitute for culture medium [J/OL]. Journal of Environmental Science, 1-16 [2025-05-24]. https://doi.org/10.13671/j.hjkxxb.2025.0069.
35. FU Hao. Effects of common oral bacterial infections on periodontal disease [J]. Industrial Microbiology, 2025,55(02):156-158.
36. Li Jiwei, Liu Xiaolan, Zheng Xiqun, et al. Research progress on the preparation of erythritol by microbial fermentation [J/OL]. Food and Fermentation Industry, 1-10

[2025-05-24]. HTTPS://doi.org/10.13995/J. CN Ki.11-1802/TS.042633.

37. Song Yan, Yao Kaiyue, Xu Jing, et al. Effects of extracellular polysaccharides of sphingomonas on oleic acid-induced glucolipid metabolic disorders in IR-HepG2 cells [J/OL]. Acta Microbiologica Sinica, 1-21 [2025-05-24]. https://doi.org/10.13343/j.cnki.wsxb.20240813.
38. Liang SX, Zhang Chen, Li BQ, et al. The negative regulatory effect of ScvL on the biofilm formation of vibrio parahaemolyticus [J/OL]. Journal of Aquatic Biology, 1-9 [2025-05-24]. http://kns.cnki.net/kCMS/detail/42.1230.q.20250520.0956.002.html.
39. Yu Qunfang, Zhang He, Qi Yanxiang, et al. Whole genome sequencing and comparative genomic analysis of XcmL5, a pathogen of mango bacterial black spot [J/OL]. Molecular Plant Breeding, 1-23 [2025-05-24]. http://kns.cnki.net/kcms/detail/46.1068.s.20250520.1105.002.html.
40. Li Shuangxiong, Yao Tuo, Chai Jiali, et al. effect of that addition of compound microbial inoculum on the physicochemical property of degraded alpine meadow soil [J/OL]. grassland and turfgrass, 1-13 [2025-05-24]. http://kns. cnki. net/kcms/detail/62.1156. S. 20250519. 1357. 002. html.
41. Wu Yating, Liu Yu, Meilin. Effects of Pediococcus lactis S1 on the antioxidant activity of myofibrillar protein [J/OL]. Journal of Anhui Agricultural University, 1-9 [2025-05-24]. https://doi.org/10.13610/j.cnki.1672-352x.20250519.020.
42. Wang Xue, Qiu Dai-Yu, Jiang Kan, et al. Effects of microbial fertilizer on root nutrient content, yield and quality of Radix et Rhizoma Glycyrrhizae [J/OL]. grassland science, 1-16 [2025-05-24]. http://kns.cnki.net/kcms/detail/62.1069.s.202505517.1445.004.html.
43. Zhang Li, Cui Yaoming, Wang Qiumei, et al. Study on the effect of probiotics on promoting the proliferation and differentiation of intestinal epithelial cells [J/OL]. Feed Research, 1-13 [2025-05-24]. http://kns.cnki.net/kcms/detail/11.2114.s.20250514.1528.002.html.
44. Chen Genwang, Liu Lei, Huang Jiaming, et al. In vitro inhibitory effect of extracts of plantain on biofilm formation of *Staphylococcus aureus* [J]. Jilin Medical

Science, 2025,46(05):1025-1028.

45. LI Shu-ya, WU Yi-qing, Zhang Liping, et al. Screening of Co-cultured Lactic Acid Bacteria from a Metabolic Perspective and Study on Its Mechanism [J/OL]. Food and Fermentation Industry, 1-14 [2025-05-24]. HTTPS://DOI.org/10.13995/J. CN Ki.11-1802/TS.042363.
46. Li Zhongyang, Ma Shifeng, Geng Shixia, et al. Research progress on preparation technology of bioactive peptides and their application in aquatic feed [J]. Feed Industry, 2025, 46 (09): 132-141. DOI: 10.13302/J. CN KI. FI.2025.09.020.
47. GONG Xi, Zhao Yuxi, Tong Man, et al. Effects of chemical oxidation of different forms of Fe(Ⅱ) on the biological reduction of nitrate [J/OL]. Environmental Science and Technology, 1-11 [2025-05-24]. http://kns.cnki.net/kcms/detail/42.1245.x.20250509.1305.002.html.
48. Zhao Yujie, Johnny, Pan Xuewei, et al. Molecular mechanisms of CpxA/R two-component system participating in the regulation of physiological characteristics of Serratia marcescens [J/OL]. Journal of Applied and Environmental Biology, 1-18 [2025-05-24]. https://doi.org/10.19675/j. cnki.1006-687x.2024.11045.
49. LIU Bo-lang, ZHANG Yi-tian, XIAO Pan, et al. Analysis of probiotic characteristics of four strains of Lactobacillus coil isolated from Huaixiang chicken [J/OL]. Feed research, 1-23 [2025-05-24]. http://kns.cnki.net/kcms/detail/11.2114.s.20250502.1840.002.html.
50. LU Han-chi, Wen Hao, Yu Yang, et al. Research progress on biological function and application of metaplasia [J]. Journal of Food Safety and Quality Testing, 2025, 16 (09): 1-11. DOI: 10.19812/J. CN KI. JFS Q11-5956/TS.2025011601.